

UC San Diego

UC San Diego Previously Published Works

Title

Search for MSSM Higgs bosons decaying to $\mu^+\mu^-$ in proton-proton collisions at $\sqrt{s}=13\text{TeV}$

Permalink

<https://escholarship.org/uc/item/7md8r122>

Authors

Sirunyan, AM
Tumasyan, A
Adam, W
[et al.](#)

Publication Date

2019-11-10

DOI

10.1016/j.physletb.2019.134992

Peer reviewed



Search for MSSM Higgs bosons decaying to $\mu^+\mu^-$ in proton-proton collisions at $\sqrt{s} = 13$ TeV

The CMS Collaboration^{*}

CERN, Switzerland

ARTICLE INFO

Article history:

Received 6 July 2019

Received in revised form 20 September 2019

Accepted 30 September 2019

Available online 4 October 2019

Editor: M. Doser

Keywords:

CMS

Higgs

Muon

BSM

MSSM

Model independent

ABSTRACT

A search is performed for neutral non-standard-model Higgs bosons decaying to two muons in the context of the minimal supersymmetric standard model (MSSM). Proton-proton collision data recorded by the CMS experiment at the CERN Large Hadron Collider at a center-of-mass energy of 13 TeV were used, corresponding to an integrated luminosity of 35.9 fb^{-1} . The search is sensitive to neutral Higgs bosons produced via the gluon fusion process or in association with a $b\bar{b}$ quark pair. No significant deviations from the standard model expectation are observed. Upper limits at 95% confidence level are set in the context of the $m_h^{\text{mod+}}$ and phenomenological MSSM scenarios on the parameter $\tan\beta$ as a function of the mass of the pseudoscalar A boson, in the range from 130 to 600 GeV. The results are also used to set a model-independent limit on the product of the branching fraction for the decay into a muon pair and the cross section for the production of a scalar neutral boson, either via gluon fusion, or in association with b quarks, in the mass range from 130 to 1000 GeV.

© 2019 The Author(s). Published by Elsevier B.V. This is an open access article under the CC BY license (<http://creativecommons.org/licenses/by/4.0/>). Funded by SCOAP³.

1. Introduction

The boson discovered at the Large Hadron Collider (LHC) in 2012 [1–3], with a mass around 125 GeV [4], has properties that are consistent with those predicted for the standard model (SM) Higgs boson [5]. However, the SM is known to be incomplete, and several well-motivated theoretical models beyond the SM predict an extended Higgs sector. One example is supersymmetry [6,7] that protects the mass of the Higgs boson against quadratically divergent quantum corrections. In the minimal supersymmetric standard model (MSSM) [8–10], the Higgs sector consists of two Higgs doublets, one of which couples to up-type fermions and the other to down-type fermions. Assuming that CP symmetry is conserved, this results in two charged bosons H^\pm , two neutral scalar bosons, h and H, and one pseudoscalar boson, A.

At the tree level, the Higgs sector in the MSSM can be described by only two parameters, which are commonly chosen as m_A , the mass of the neutral A, and $\tan\beta$, the ratio of the vacuum expectation values of the neutral components of the two Higgs doublets. The masses of the other four Higgs bosons can be expressed as a function of these two parameters. Beyond the tree level the MSSM Higgs sector depends on additional parameters, which enter via higher-order corrections in perturbation theory, and which are

usually fixed to values motivated by experimental constraints and theoretical assumptions. Setting these parameters defines a benchmark scenario [11], which is then described by m_A and $\tan\beta$. The relevant scenarios are those consistent with a mass of one neutral boson of 125 GeV for the majority of the probed m_A - $\tan\beta$ parameter space [12], and not ruled out by other existing measurements. In particular, the $m_h^{\text{mod+}}$ scenario [11] constrains the mass of the h boson to be near 125 GeV for a wide range of $\tan\beta$ and m_A values, by tuning some of the MSSM parameters. In the phenomenological MSSM (hMSSM) [13–16] the mass of h boson is an input parameter, set to 125 GeV, and the observed neutral boson is interpreted as the h boson. Small differences in the cross sections and branching fractions exist between the two models, although the kinematics of the Higgs bosons remains almost identical.

This Letter reports on a search for beyond-the-SM neutral Higgs bosons in the dimuon final state in proton-proton (pp) collisions at a center-of-mass energy \sqrt{s} of 13 TeV. The search is performed in the context of the MSSM for values of m_A larger than 130 GeV, assuming either the $m_h^{\text{mod+}}$ or the hMSSM scenario. For values of $m_A \gtrsim 200$ GeV, the MSSM is close to the decoupling limit: the h boson takes the role of the observed SM-like Higgs boson at 125 GeV, and the H and A bosons are nearly degenerate in mass. For values of $m_A \lesssim 200$ GeV the MSSM leads to similar, but not degenerate, masses for the H and A bosons [17]. The mass of the h boson is assumed to be at 125 GeV, and its width smaller than

^{*} E-mail address: cms-publication-committee-chair@cern.ch.

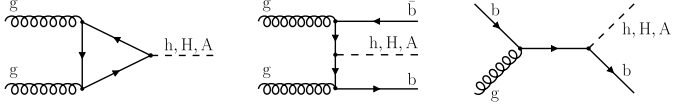


Fig. 1. Leading order Feynman diagrams for the production of the MSSM Higgs boson: gluon fusion production (left) and b-associated production (middle and right).

the experimental resolution, consistently with the ATLAS and CMS measurements in other decay modes [4,18,19]. The analysis tests the h boson production as predicted by the MSSM and the constraints on its production mechanisms measured by ATLAS and CMS are not enforced. Alternatively, the search is also performed in a model-independent way, where a neutral boson is assumed to be produced either via gluon fusion or in association with a $b\bar{b}$ quark pair.

At the LHC, dominant production mechanisms for the neutral A and H bosons are gluon fusion, in which the Higgs boson can be produced via a virtual loop of bottom or top quarks, and b-associated production, where the Higgs boson is produced in association with a b quark pair. This is also the case of the h boson for values of $m_A \lesssim 200$ GeV, while, in the decoupling regime, the h boson production mechanisms correspond to those predicted by the SM. Fig. 1 shows the Feynman diagrams for the two production processes at leading order (LO). The gluon fusion mechanism is more relevant for $\tan\beta \lesssim 30$, whereas at LO, the coupling of the Higgs boson to down-type fermions is enhanced by $\tan\beta$, resulting in b-associated production becoming more important at large $\tan\beta$. The coupling of the neutral Higgs boson to charged leptons is enhanced for the same reason. Although the branching fraction to muons is predicted to be about 300 times smaller than that for the $\tau^+\tau^-$ final state, the $\mu^+\mu^-$ channel can be fully reconstructed, and the dimuon invariant mass can be measured with a precision of a few percent by exploiting the excellent muon momentum resolution of the CMS detector, making the dimuon final state an additional probe of the MSSM.

The common experimental signature of the two production mechanisms is a pair of opposite-charge muons with high transverse momentum (p_T). The b-associated production process is characterized by the presence of additional jets originating from b quark fragmentation, whereas the events containing jets from light quarks or gluons are linked to the gluon fusion production mechanism. The presence of a signal would be characterized by an excess of events over the SM background in the dimuon invariant mass corresponding to the value of the Higgs boson masses.

The analysis is performed using the data at $\sqrt{s} = 13$ TeV collected during 2016 by the CMS experiment at the LHC corresponding to an integrated luminosity of 35.9 fb^{-1} . Similar searches in the dimuon final state were performed by the ATLAS and CMS Collaborations using data collected in pp collisions at 7 and 8 TeV [20, 21], and by ATLAS at 13 TeV [22]. Searches for neutral Higgs bosons in the framework of the MSSM were performed by the ATLAS and CMS experiments also in the $\tau^+\tau^-$ [20,23–28] and $b\bar{b}$ [29–31] final states. Limits on the existence of the MSSM Higgs bosons were determined also in e^+e^- collisions at $\sqrt{s} = 91\text{--}209$ GeV at the CERN LEP [32] and in proton-antiproton collisions at $\sqrt{s} = 1.96$ TeV at the Fermilab Tevatron [33–36].

2. The CMS detector

The central feature of the CMS apparatus is a superconducting solenoid of 6 m internal diameter, providing a field of 3.8 T. Within the field volume are a silicon pixel and strip tracker, a crystal electromagnetic calorimeter (ECAL), and a brass and scintillator hadron calorimeter (HCAL), each composed of a barrel and two endcap

sections. Muons are measured in gas-ionization detectors embedded in the steel return yoke of the magnet. The first level (L1) of the CMS trigger system uses information from the calorimeters and muon detectors to select events of interest. The high-level trigger processor farm decreases the L1 accept rate from around 100 kHz to about 1 kHz before data storage. A more detailed description of the CMS detector, together with a description of the coordinate system and main kinematic variables used in the analysis, can be found in Ref. [37].

3. Signal and background simulation

Samples of Monte Carlo (MC) simulated events are generated to model the Higgs bosons signal for the two leading production processes. This is done for a large number of m_A and $\tan\beta$ combinations, where m_A spans the range from 130 to 1000 GeV and $\tan\beta$ is varied from 5 to 60. Higgs boson events are generated with a mass within $\pm 3\Gamma$ of the nominal Higgs boson mass, where Γ is the intrinsic width. The values of Γ strongly depend on m_A and $\tan\beta$, being, for example, $\Gamma = 0.2$ (2.7)% of the nominal Higgs boson mass at $m_A = 150$ (550) GeV and $\tan\beta = 10$ (40). The signal samples are generated with PYTHIA 8.212 [38] at LO. Additional signal samples are generated at next-to-LO (NLO) for some mass points to estimate higher-order corrections: gluon fusion samples are produced with POWHEG 2.0 [39], while b-associated production samples are produced with MADGRAPH5_AMC@NLO [40] using the four-flavor scheme.

Simulated background processes are used to optimize the event selection but not to model the background shape and normalization, which are determined directly from data. The most relevant SM background processes considered are Drell–Yan (DY) production, and single and pair production of top quarks, which can produce $\mu^+\mu^-$ pairs with large invariant mass. Other background sources are the diboson production processes, $W^\pm W^\mp$, $W^\pm Z$, and ZZ , whose contributions are each smaller than 1% for dimuon invariant masses larger than 130 GeV, the Higgs boson search region. The background samples are generated at NLO using MADGRAPH5_AMC@NLO and POWHEG. Spin correlations in multi-boson processes generated using MADGRAPH5_AMC@NLO are simulated using MADSPIN [41]. The NNPDF 3.0 [42] parton distribution functions (PDFs) are used for all samples. The parton shower and hadronization processes are modeled by PYTHIA with the CUETP8M1 [43] underlying event tune.

Detector response is based on a detailed description of the CMS detector and is simulated with the GEANT4 package [44]. Additional pp interactions in the same or nearby bunch crossings (pileup) are simulated by PYTHIA. During the data taking period, the CMS experiment was operating with, on average, 23 inelastic pp collisions per bunch crossing. The distribution of the number of additional interactions per bunch crossing in the simulation is weighted to match that observed in the data.

The values of the Higgs boson masses, widths, and the Yukawa couplings are calculated as a function of m_A and $\tan\beta$ following the LHC Higgs Cross Section Working Group prescriptions [45,46], using the FEYNHIGGS 2.12.0 [47–51] program for the $m_h^{\text{mod}+}$ scenario. The inclusive cross sections of the Higgs bosons for the gluon fusion process are obtained with SusHi [52], which includes NLO supersymmetric-QCD corrections [53–58], next-to-NLO (NNLO) QCD corrections for the top-quark contribution in the effective theory of a heavy top quark [59–63], and electroweak effects by light quarks [64,65]. Higgs boson cross sections for the b-associated production are calculated with SusHi, and rely on matched predictions [66], which are based on the five flavor NNLO QCD calculation [67] and the four flavor NLO QCD calculation [68,69]. Higgs to $\mu^+\mu^-$ branching fractions are calculated with

FEYNHIGGS for the $m_h^{\text{mod+}}$ scenario and using the program HDECAY 6.40 [70] for the hMSSM scenario. Cross sections for the $t\bar{t}$ and DY background processes are computed at the NNLO with TOP++2.0 [71] and FEWZ3.1 [72], respectively, while for the single top and the diboson production processes they are computed at NLO with HATHOR [73,74] and MCFM [75], respectively.

4. Object reconstruction and event selection

The particle-flow (PF) algorithm [76] aims at reconstructing and identifying each individual particle in an event, with an optimized combination of information from the various elements of the CMS detector. The energy of photons is obtained from the ECAL measurement. The energy of electrons is obtained from a combination of the electron momentum at the primary interaction vertex as determined by the tracker, the energy of the corresponding ECAL cluster, and the energy sum of all bremsstrahlung photons spatially compatible with originating from the electron track. The energy of muons is obtained from the curvature of the corresponding track. The energy of charged hadrons is determined from a combination of their momentum measured in the tracker and the matching ECAL and HCAL energy deposits, corrected for zero-suppression effects and for the response function of the calorimeters to hadronic showers. Finally, the energy of neutral hadrons is obtained from the corresponding corrected ECAL and HCAL energies.

Muons with $20 < p_T < 100 \text{ GeV}$ are measured with a relative p_T resolution of 1.3 to 2% in the barrel and better than 6% in the endcaps. The p_T resolution in the barrel is better than 10% for muons with p_T up to 1 TeV [77,78].

Jets are reconstructed using the anti- k_T clustering algorithm [79] with a distance parameter of 0.4, as implemented in the FASTJET package [80]. The quantity missing transverse momentum, p_T^{miss} , is defined as the magnitude of the negative vector p_T sum of all the PF objects (charged and neutral) in the event, and is modified by corrections to the energy scale of reconstructed jets. Collision vertices are obtained from reconstructed tracks using a deterministic annealing algorithm [81]. The reconstructed vertex with the largest value of summed physics-object p_T^2 is taken to be the primary pp interaction vertex (PV). The physics objects are the jets, clustered using the jet finding algorithm [79,80] with the tracks assigned to the vertex as inputs, and the associated missing transverse momentum taken as the negative vector sum of the p_T of those jets.

The combined secondary vertex algorithm of Ref. [82] is used to identify jets resulting from the hadronization of b quarks. A medium operating working point of the algorithm is applied to jets with $p_T > 20 \text{ GeV}$ in the pseudorapidity range $|\eta| < 2.4$. Within this kinematic range, the efficiency of the algorithm is 66% with a misidentification probability of 1%.

The events are preselected by the trigger system [83] requiring a muon candidate with $|\eta| < 2.4$, satisfying at least one of the following criteria: $p_T > 24 \text{ GeV}$ with isolation (iso) requirements, or $p_T > 50 \text{ GeV}$ without isolation requirements. These are the trigger algorithms with the lowest p_T threshold whose output is not artificially reduced to limit the event rate and that cover the entire η acceptance of the muon detector. Since the Higgs boson signal is searched for over a large mass range, the p_T of the muons from its decay can vary from tens to hundreds of GeV. Therefore, two sets of muon identification (ID) criteria are employed in the analysis: one is optimized for muons with lower p_T ($\lesssim 200 \text{ GeV}$) (ID1) and the other for muons with larger p_T (ID2).

Events with a pair of opposite-charge muons, coming from the PV, are selected requiring both muons to satisfy the same ID criterion. Accepting, more generally, pairs of muons that pass any of

Table 1

Summary of the muon selection criteria.

Muon selection	muon ID1	muon ID2
Online selection:	$ \eta < 2.4$	$ \eta < 2.4$
Single muon	$p_T > 24 \text{ GeV}$	$p_T > 50 \text{ GeV}$
	Online iso	
Offline selection:	$ \eta < 2.4$	$ \eta < 2.4$
Two opposite-charge muons	$p_T > 26 \text{ GeV}$	$p_T > 53 \text{ GeV}$
	Offline iso1 < 0.25	offline iso2 < 0.1

the two ID criteria would lead to a negligible increase in signal efficiency. At least one of the two muon candidates has to match (in η and azimuthal angle ϕ in radians) the muon that triggered the event. The trigger requirement depends on the ID algorithm. Offline reconstructed muons with $|\eta| < 2.4$ are considered. Their offline p_T is required to be higher than 26 or 53 GeV, to be compatible with the muon that triggered the event. To reject muons from nonprompt decays, muon candidates must be isolated. The offline isolation variable is calculated depending on the ID algorithm, and is labeled iso1 (iso2) for ID1 (ID2). For ID1 it is the scalar p_T sum of the PF charged and neutral hadrons in a cone of radius $\Delta R = \sqrt{(\Delta\eta)^2 + (\Delta\phi)^2} = 0.4$ around the muon direction, divided by the muon p_T . The charged PF particles not associated with the PV are not considered in this sum, and a correction is applied in order to account for the neutral particle contamination arising from pileup [84]. For ID2 the offline iso is computed as the scalar p_T sum of tracks in the silicon tracker, excluding the muon, in a cone of radius $\Delta R = 0.3$ around the muon direction, and divided by the muon p_T . Tracks not associated with the PV are not considered. Energy deposits in the calorimeters are not included, since electromagnetic showers can develop from photons radiated by a high- p_T muon. The invariant mass of the Higgs boson candidate is reconstructed from the two highest- p_T opposite-charge muon candidates in the event. The dimuon selection criteria are summarized in Table 1.

The muon momentum measurement is crucial for the reconstruction of the Higgs boson mass peaks since improving the dimuon mass resolution increases the sensitivity of the analysis. To set limits accurately, the mean and the resolution of the dimuon mass peaks in simulation must match those of the data. A correction of the muon momentum has been applied in order to provide consistent measurements in the different ϕ and η regions of the detector, improving the net resolution in data. The correction [78] is also applied to the simulated muons to align the scale and resolution to those measured in the data. The magnitudes of the momentum scale corrections are about 0.2 and 0.3% in the barrel and endcaps, respectively, for muons with p_T up to 200 GeV. For muons with larger p_T , since the statistical precision of the data is too poor to derive a correction, only a systematic uncertainty is considered (see Section 5).

When the Higgs boson is produced in association with a $b\bar{b}$ pair, additional jets from b quark fragmentation are expected. Jets with $p_T > 20 \text{ GeV}$ and $|\eta| < 2.4$ are considered in this analysis: those that satisfy the requirements for the medium b-tagging working point [82] are taken as b-jet candidates, otherwise they are taken as untagged jets. Events containing b-jet candidates provide the highest sensitivity for the b-associated production channel, and events that do not contain b-tagged jets provide the best sensitivity for the gluon fusion production channel. The events are therefore split into two exclusive categories: the b-tag category, containing events with strictly one b jet and at most one additional untagged jet, and the no-b-tag category, containing events without b-tagged jets. In the first category, the requirement of strictly one b jet is aimed at suppressing about 30% of the dominant background from top quark pairs, since the observed b-tagged

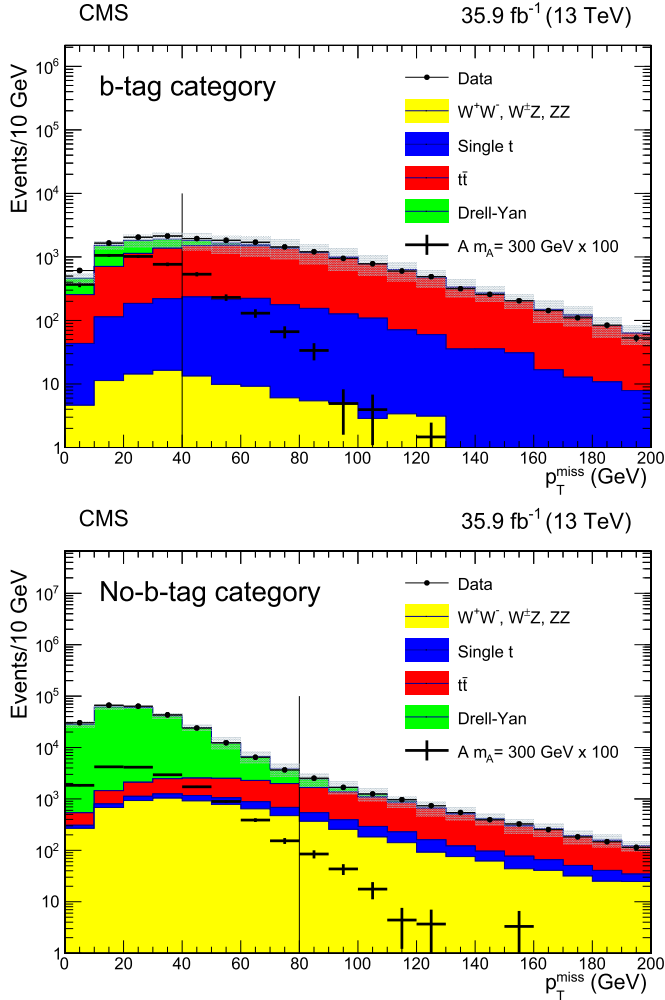


Fig. 2. Distribution of the missing transverse momentum in (upper) b-tag and (lower) no-b-tag categories, for events with dimuon invariant mass larger than 130 GeV, as observed in data (dots) and predicted by simulation (colored histograms). The shaded gray band around the total background histogram represents the total uncertainty in the simulated prediction. The contribution of the expected signal for $m_A = 300$ GeV and $\tan\beta = 20$, scaled by a factor of 100, is superimposed for illustration. The vertical line represents the upper threshold used to select the events in the two categories.

jet multiplicity in $t\bar{t}$ events is on average higher than for the Higgs boson signal. This is because more than half of the signal events from b-associated production are characterized by b jets emitted at large η , out of the acceptance of the tracking detector, and failing the b-tag requirements, whereas b jets in $t\bar{t}$ events are preferentially emitted in the central η region. Therefore, discarding events with two or more b-tagged jets allows the $t\bar{t}$ background to be rejected without any major impact on the signal efficiency. Furthermore, $t\bar{t}$ events are characterized by a higher multiplicity of additional untagged jets than the signal events.

Signal events are characterized by a rather small p_T^{miss} . However, the background content is quite different for the two categories, as shown in Fig. 2. The background from $t\bar{t}$ events, characterized by a relatively large p_T^{miss} from W boson decays, is much more relevant for the b-tag category. For the no-b-tag category, the dominant background is DY production, whose events are characterized by a p_T^{miss} distribution that is similar to that of the signal. For this reason, a requirement on p_T^{miss} , separately tuned for the b-tag and the no-b-tag events, improves the background rejection and increases the signal sensitivity. Events belonging to the b-tag

Table 2

Summary of the selection criteria that define the two event categories. Categorization is applied after the muon selection.

	b-tag category	No-b-tag category
b-tagged jets	1 with $p_T > 20$ GeV, $ \eta < 2.4$	Veto
Untagged jets	0,1 with $p_T > 20$ GeV, $ \eta < 2.4$	
p_T^{miss}	< 40 GeV	< 80 GeV

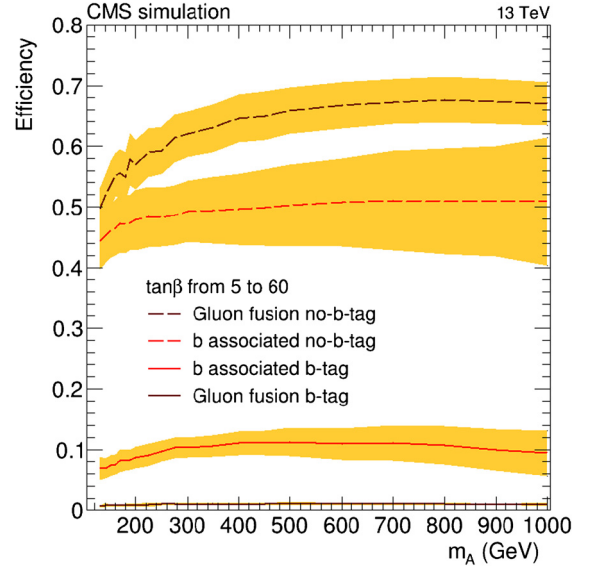


Fig. 3. The selection efficiency for the A boson, as a function of its mass, for the two production mechanisms, b-associated and gluon fusion, and for each of the two event categories. The band centered on each curve corresponds to the envelope of efficiencies obtained when varying $\tan\beta$, combined with the statistical and systematic uncertainties.

(no-b-tag) category are required to have $p_T^{\text{miss}} < 40$ (80) GeV. This requirement reduces the background from top quark production by about 75% (40%). The selection criteria that define the two categories are summarized in Table 2.

5. Signal efficiency and signal systematic uncertainties

For each value of m_A and $\tan\beta$, the signal efficiency for each Higgs boson sample is defined as the fraction of generated events that fulfill the selection criteria. This definition of efficiency also includes the effects of limited detector acceptance and the selections outlined in Section 4.

Fig. 3 shows the selection efficiency for the A boson as a function of m_A , for the gluon fusion and the b-associated production processes, and for the two event categories. Each curve corresponds to the mean of the efficiency obtained by varying $\tan\beta$ between 5 and 60, while the band of each curve corresponds to the efficiency variations combined with the statistical and systematic uncertainties (described in the next paragraph) of the simulated samples. For a given mass, the selection efficiency is weakly dependent on $\tan\beta$, since this parameter mostly affects the Higgs boson width, with a negligible impact on the kinematic properties of the event. The efficiency to detect events produced in association with b quarks is approximately 10% at high masses for the b-tag category. This value is mostly determined by the large fraction of b jets that are emitted with an η value that is outside the coverage of the tracking detectors, and indeed $\approx 50\%$ of events from b-associated samples are reconstructed in the no-b-tag category. The efficiency to detect events from gluon fusion reaches a maximal value at $\approx 65\%$ for $m_A \gtrsim 400$ GeV. The very small but

Table 3

Systematic uncertainties in the signal efficiency for the two event categories. The systematic uncertainties hold for both Higgs boson production processes except for the sources listed in the last three rows, which apply to the b-associated production process only. For these three sources, in the model-independent search for a neutral boson produced in association with b quarks, the uncertainties are applied as quoted in the table. In the MSSM interpretation, these numbers have to be weighted by the relative contribution of the b-associated production process to each category. For those sources of systematics that depend on m_A the range of uncertainty is quoted.

Source	Systematic uncertainty (%)	
	b-tag category	No-b-tag category
MC statistical uncertainty	0.5–6	0.2–2
Trigger efficiency	0.9	0.9
Muon reconstruction	2	2
Muon isolation	1	2
Pileup	0.8	0.9
Jet energy scale	1.6	0.4
Unclustered energy	4.1	0.3
PDF	3	3
Higgs boson p_T	1–4	1–4
b tag (only for b-associated production)	2	0.6
b jet multiplicity (only for b-associated production)	20–30	7–20
Untagged jet multiplicity (only for b-associated production)	7–25	–

nonvanishing efficiency for signal produced via gluon fusion in the b-tag category is due to the b misidentification probability, which is about 1%. The corresponding efficiencies for the H boson are consistent with those shown in Fig. 3.

The systematic uncertainties in the signal description arise from a possible mismodeling of the signal efficiency, of the signal shape, and, for the model interpretation, from uncertainties in its cross section.

The systematic uncertainties that affect the signal efficiency are given in Table 3. The size of the simulated signal samples introduces a statistical uncertainty in the signal efficiency that is between 0.2% and 6%, depending on the number of generated events.

In order to account for the differences between data and simulation in the muon trigger efficiency, identification, and isolation, scale factors calculated using the tag-and-probe technique [77,78] have been applied to simulated events. A similar procedure is used to account for discrepancies between data and simulation in the b-tagging efficiency. A global correction, calculated as the product of the various scale factors, is applied as an event-by-event weight. The uncertainty associated with each scale factor is then propagated to the analysis and its impact on the final selection efficiency is assigned as systematic uncertainty. An event-by-event weight is also applied to account for the modeling of the pileup in the simulation. The uncertainty in the knowledge of the pileup multiplicity is evaluated by varying the total inelastic cross section [85,86] by $\pm 5\%$, which translates into an uncertainty smaller than 1% in the signal efficiency. The uncertainty associated with the jet energy scale [87] is estimated by rescaling the jet momentum by a factor depending on the p_T and η of each jet. This variation is also propagated to the p_T^{miss} determination. Its effect on the signal selection efficiency is about 1.6 (0.4)% for the b-tag (no-b-tag) category. Systematic uncertainties in the unclustered energy are propagated to the determination of p_T^{miss} . The effect on the signal efficiency is 4.1% for the b-tag category, and 0.3% for the no-b-tag category. Systematic uncertainty in the b-tagging algorithm affects the signal yield and the category migration with an impact on the signal efficiency of 2% for the b-tag category and 0.6% for the no-b-tag category. The uncertainty in the total integrated luminosity is 2.5% [88] and affects the signal yield.

The uncertainties in the MSSM cross sections depend on m_A , $\tan\beta$, and the scenario. They are provided by the LHC Higgs Cross Section Working Group [45,46]. An uncertainty of 3% is used to account for the parton distribution functions.

Additional corrections are applied to take into account the fact that the signal samples are generated with PYTHIA at LO instead of using an NLO generator. Higher-order corrections affect the Higgs boson p_T modeling, with impacts on the muon acceptance and the jet multiplicity. Moreover, they cause event migration between the two categories. The acceptance obtained from the LO samples is corrected to that predicted at NLO. The corresponding systematic uncertainty is set to the size of the correction itself. The correction on the modeling of the Higgs p_T increases the signal efficiency by 1–4%, depending on the Higgs boson mass. The correction on the b-jet multiplicity affects only the b-associated signal, resulting in a correction of 20–30% depending on m_A , which increases the signal efficiency for the b-tag category, and a correction of 7–20% decreasing the signal efficiency for the no-b-tag category. An additional correction of 7–25%, related to the untagged jet multiplicity, is applied, and reduces the signal efficiency for the b-tag category, due to the veto on the untagged jets.

The systematic uncertainties in the b-tag efficiency and the jet multiplicity shown in Table 3 apply only to the b-associated production process. Both the b-tagging and the b-jet multiplicity uncertainties are anticorrelated between the two event categories. In the model-independent analysis for the case in which the neutral boson is assumed to be entirely produced in association with b quarks, these uncertainties are applied, as quoted in Table 3, while in the MSSM interpretation, where both the gluon fusion and the b-associated production processes contribute to the two event categories, these systematic uncertainties are weighted by the relative contribution of the latter process.

The shape of the reconstructed Higgs boson invariant mass distribution is affected by the muon momentum scale and resolution. Uncertainties in the calibration of these quantities are propagated to the shape of the invariant mass distribution assuming a Gaussian prior, leading to a variation of up to 10% in the width of the signal mass peak, and to a negligible shift of its position. These uncertainties are taken into account as a signal shape variation in the calculation of the exclusion limit.

6. Modeling of the signal and background shapes

The invariant mass spectrum of the signal events that pass the event selection is used to determine the signal yield for each category. In the framework of the MSSM, this is done by fitting the invariant mass distribution of the h, H, and A bosons, separately for the two event categories and for various combinations of

m_A - $\tan\beta$ values. The function F_{sig} used to parametrize the signal mass shape [21] is defined as:

$$F_{\text{sig}} = w_h F_h + w_H F_H + w_A F_A. \quad (1)$$

In Eq. (1), the terms F_h , F_H , and F_A describe the mass shape of the h, H, and A signals, respectively. Each term is a convolution of a Breit-Wigner (BW) function to describe the resonance, with a Gaussian function to account for the detector resolution. The two parameters of the BW function, as well as the variance of each Gaussian function, are free parameters of the fit used to determine the signal model, while the quantities w_h , w_H , and w_A are the numbers of expected events for each boson passing the event selection. For the m_A - $\tan\beta$ points for which the signal samples were not generated, the parameters are interpolated from the nearby generated points. In order to correct for differences of the order of a few GeV between the PYTHIA prediction of m_H with respect to the value calculated by FEYNHIGGS in the $m_h^{\text{mod+}}$ or the value used in the hMSSM, especially for $m_A \lesssim 200$ GeV, the invariant mass distribution of the H boson is shifted by the corresponding amount. For the model-independent analysis the signal shape is described using one single resonance in Eq. (1).

The analysis does not use background estimation from simulation due to the limited size of simulated events compared to data in the region of interest, as well as due to the large theoretical uncertainties in the background description at high invariant masses. Therefore, given the smooth dependence of the background shape on the dimuon invariant mass, it is estimated from the data, by assuming a functional form to describe its dependence as a function of the reconstructed dimuon invariant mass, $m_{\mu\mu}$, and by fitting it to the observed distribution.

The functional form used to describe the background shape is defined as:

$$F_{\text{bkg}} = \exp(\lambda m_{\mu\mu}) \times \left[\frac{f}{N_1} \frac{1}{(m_{\mu\mu} - m_Z)^2 + \frac{\Gamma_Z^2}{4}} + \frac{(1-f)}{N_2} \frac{1}{m_{\mu\mu}^2} \right]. \quad (2)$$

The quantity $\exp(\lambda m_{\mu\mu})$ parametrizes the exponential part of the mass distribution, and f represents the weight of the BW term with respect to DY photon exchange, while N_1 and N_2 correspond to the integral of each term in F_{bkg} . The quantities λ and f are free parameters of the fit. The parameters Γ_Z and m_Z are separately determined for the two event categories by fitting the dimuon mass distribution close to the Z boson mass. The fit provides the effective values of such quantities, which include detector and resolution effects. Their values are then kept constant when using F_{bkg} in the final fit. The systematic uncertainty that stems from the choice of the functional form in Eq. (2), which was used in earlier searches [21], is assessed as described below.

A linear combination of the functions describing the expected signal and the background is then used to perform a binned maximum likelihood fit to the data, where the uncertainties are treated as nuisance parameters:

$$F_{\text{fit}} = (1 - f_{\text{bkg}}) F_{\text{sig}} + f_{\text{bkg}} F_{\text{bkg}}. \quad (3)$$

The fit is performed for each m_A and $\tan\beta$ hypothesis, as the yield of the signal events and the shape of F_{sig} depend on these quantities. The parameters that describe the signal are determined by fitting the simulated samples that pass the event selection with Eq. (1), for each m_A and $\tan\beta$ pair, as explained above. Subsequently they are assigned as constant terms in F_{fit} . The quantity f_{bkg} is a free parameter in the fit, and the fraction of signal events

is defined as $f_{\text{sig}} = (1 - f_{\text{bkg}})$. The overall normalization is also a free parameter and is profiled in the fit.

For each m_A assumption, the function F_{fit} is used to fit the data over an $m_{\mu\mu}$ range centered on m_A . The range has to be large enough to account for the signal width, including the experimental resolution, and it is ± 50 GeV for $m_A \leq 290$ GeV, ± 75 GeV for $290 < m_A \leq 390$ GeV, and ± 100 GeV for $390 < m_A \leq 500$ GeV. For values of m_A smaller than 165 GeV the lower bound of the mass window is set to 115 GeV. For $m_A > 500$ GeV, the entire range from 400 to 1200 GeV is used. The h boson is used to constrain the results when its mass is included in the fitted mass range.

The uncertainty introduced by the choice of the analytical function used to parametrize the background is estimated by using a method similar to that used in Refs. [3,21,89]. The method is based on the determination of the number of spurious signal events that are introduced by the choice of the background function F_{bkg} , when the background is fit by the function F_{fit} . The invariant mass spectrum is fitted by the function F_{bkg}^a , chosen among various functional forms: Eq. (2) or other similar expressions that include a BW plus exponentials, and sum of exponentials. All these functional forms adequately describe the background distribution observed in data. The fit is performed in the proper mass range centered around the assumed value of m_A , and the parameters of F_{bkg}^a are determined. Then, thousands of MC pseudo-experiments are generated, each one containing the same number of events as observed in the data, distributed according to the functional form F_{bkg}^a . For each pseudo-experiment, the invariant mass distribution is then fit with the function F_{fit} of Eq. (3), once using F_{bkg}^a , and then using a different function F_{bkg}^b , given by Eq. (2). For each pseudo-experiment, the spurious signal yield, expressed by the number of events N_{bias}^a and N_{bias}^b , is determined. The quantity N_{bias}^a is on average consistent with zero within statistical fluctuations. The quantity N_{bias}^b represents the number of spurious signal events that are found in the signal yield if the function F_{bkg}^b is used to describe the background, when the background itself is actually distributed according to F_{bkg}^a . The median of the distribution of the difference $N_{\text{bias}}^a - N_{\text{bias}}^b$ obtained from the pseudo-experiments is defined as the bias introduced by using the function F_{bkg}^b , relative to the tested mass m_A . This procedure is repeated for each function F_{bkg}^a among the functional forms mentioned above, and the largest bias is taken as the systematic uncertainty in the number of signal events obtained from the maximum likelihood fit, due to the choice of Eq. (2) to parametrize the background distribution. Choosing a different function F_{bkg}^b , instead of Eq. (2), was shown to lead to similar biases over the whole mass range. The number of spurious signal events varies between a few units and a few hundred depending on the mass of the signal and the event category. Although the bias is due to the modeling of the background, its impact on the result depends on the expected signal strength and shape, both varying according to m_A and $\tan\beta$ in the model-dependent analysis, and according to the mass of a generic resonance ϕ for the model-independent case. More details about the effect of the bias on the final results are discussed in Section 7.

An example of fits to the data with Eq. (3), for the model-independent case, is shown in Fig. 4. Two mass hypotheses, 400 and 980 GeV, are assumed for a single narrow-width resonance ϕ decaying to two muons. The two event categories are combined according to their sensitivity, $S/(S+B)$, where S and B are the number of events in the expected signal and observed background, respectively. The uncertainties in the integrated luminosity, in the signal efficiency, and in the background parametrization are taken into account as nuisance parameters.

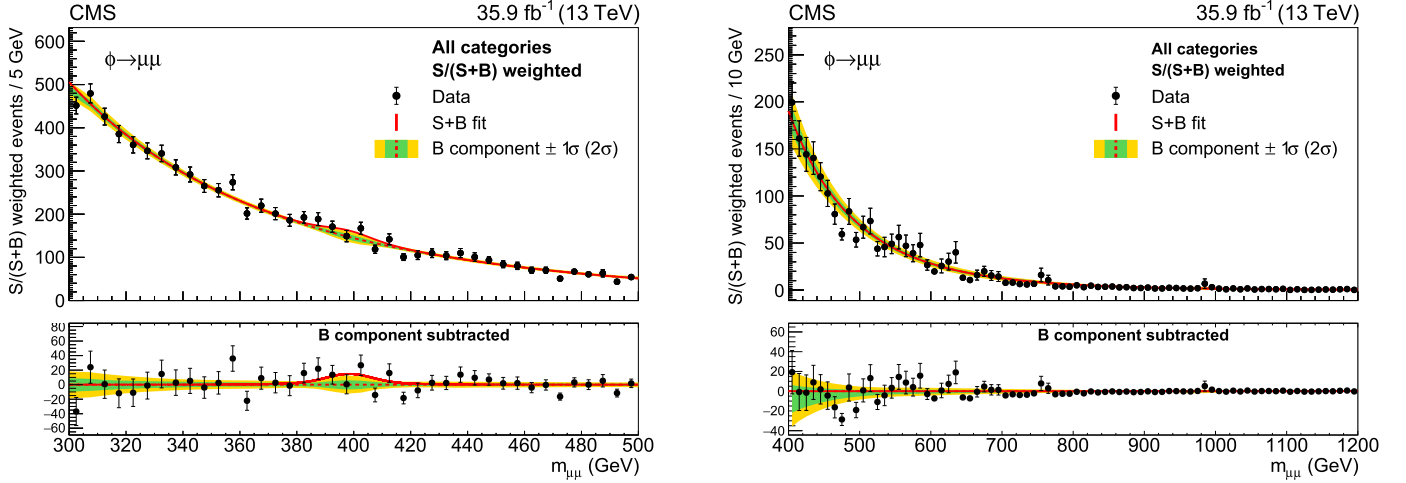


Fig. 4. Examples of fits to data with a signal plus background hypothesis, for a narrow-width signal with a mass of 400 GeV (left), and 980 GeV (right), for the two event categories added together, after weighting by their sensitivity. The resonance ϕ is assumed to be produced via the b-associated production, and to decay to two muons. The 68 and 95% CL bands, shown in dark green and light yellow, respectively, include the uncertainties in the background component of the fit. The lower panel shows the difference between the data and the background component of the fit.

7. Results

No evidence of Higgs boson production beyond the SM prediction is observed in the mass range in which the analysis has been performed. Exclusion limits at 95% confidence level (CL) are therefore determined.

A maximum likelihood fit to the data, as explained in the previous section, is performed under the background only and the signal-plus-background hypotheses, where the background includes the expectation for the SM Higgs boson. The systematic uncertainties are incorporated as nuisance parameters in the likelihood. The upper limits for the signal production are computed using the CL_s [90,91] criterion and the hybrid frequentist-bayesian approach, where the distributions of the test-statistic are derived from pseudo-experiments [92].

The results are interpreted within the MSSM in the context of the $m_h^{\text{mod}+}$ and hMSSM scenarios, by combining both event categories. The 95% CL limit on the parameter $\tan\beta$ is presented as a function of m_A : the exclusion limit is chosen for each m_A as the $\tan\beta$ value at which the CL_s is lower than 0.05.

To estimate the impact of the various systematic uncertainties, the 95% CL limits have been determined by including different combination of uncertainties: statistical plus all systematic uncertainties, statistical plus systematic uncertainties in the fit bias, statistical plus systematic uncertainties in the efficiency. The comparison shows that the systematic uncertainties pertaining to the selection efficiency and the fit bias have similar impact.

The results in terms of the expected 95% CL upper limit on the $m_h^{\text{mod}+}$ MSSM scenario (with the higgsino mass parameter $\mu = 200$), including the 68 and 95% CL bands, are shown in Fig. 5 (upper), in the m_A - $\tan\beta$ plane. The results are obtained including the statistical and all systematic uncertainties. The 95% CL upper limit is computed up to $m_A = 600$ GeV, where the excluded $\tan\beta$ value exceeds 50. For higher values of $\tan\beta$ the MSSM predictions are no longer reliable. These results extend the excluded $\tan\beta$ range obtained at 7 and 8 TeV [21] and also extend the range of the tested m_A values from 300 to 600 GeV. The data are also interpreted in terms of the hMSSM model. The corresponding 95% CL upper limit on $\tan\beta$ as a function of m_A are shown in Fig. 5 (lower). The observed limits are very similar in the two scenarios, since, in the m_A - $\tan\beta$ range covered by this analysis the $m_h^{\text{mod}+}$ predictions for the h boson mass are consistent with the SM Higgs

boson mass, and the cross sections of the H and A bosons are similar between the two models.

The results of the $\tau^+\tau^-$ analysis [28] exclude a much larger m_A - $\tan\beta$ region, reaching the value of $\tan\beta = 60$ at $m_A = 1.5$ TeV. For values of m_A up to 400 GeV the $\mu^+\mu^-$ results exclude a larger m_A - $\tan\beta$ region compared to the results of the $b\bar{b}$ analysis [31], which is instead slightly more sensitive at higher m_A reaching the value of $\tan\beta = 60$ at about $m_A = 700$ GeV.

Limits on the production cross section times decay branching fraction $\sigma\mathcal{B}(\phi \rightarrow \mu^+\mu^-)$ for a single neutral scalar boson ϕ have also been determined. In the model-independent interpretation the ϕ boson is searched for as a single resonance with mass m_ϕ assuming a narrow width or a width equal to 10% of m_ϕ . In the first case the intrinsic width of the signal is smaller than the invariant mass resolution, while in the second case the width is larger even for mass values near 1000 GeV (lower sensitivity of the analysis). The simulated signal of the A boson in the $\tan\beta = 5$ case (smallest intrinsic width, dominated by the detector resolution) is used as a template to compute the detection efficiency of a generic ϕ boson decaying to a muon pair. The ϕ boson is assumed to be produced entirely either via the b-associated or the gluon fusion process, and the analysis is performed separately for the two production mechanisms. Fig. 6 shows the 95% CL upper limits on the cross section times the decay branching fraction to $\mu^+\mu^-$ as a function of the ϕ mass for a narrow resonance. These limits are more stringent by a factor of 2 to 3 than those recently obtained by ATLAS in a similar search [22]. The corresponding upper limits assuming a signal template with a width equal to 10% of its mass value are shown in Fig. 7. In the case of large signal widths, the upper limits as a function of m_ϕ start from 140 GeV. This is done to have the signal peak $\pm 3\Gamma$ within the fit range. Moreover, as one may expect, the limits are less stringent than for the narrow-width approximation, and it is no longer possible to distinguish the fine structure of the 95% CL limits as a function of the mass, as observed for the narrow-width case.

8. Summary

A search for neutral minimal supersymmetric standard model (MSSM) Higgs bosons decaying to $\mu^+\mu^-$ was performed using 13 TeV data collected in proton-proton collisions by the CMS experiment at the LHC. No excess of events was found above the ex-

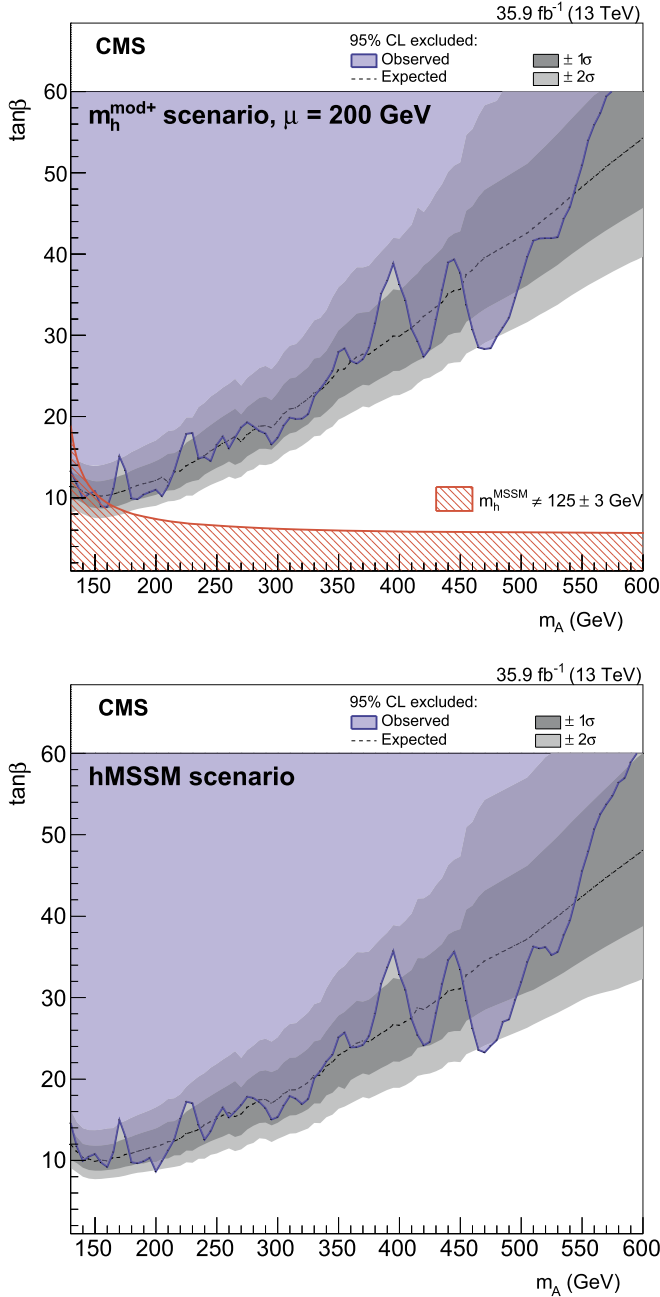


Fig. 5. The 95% CL expected, including the 68 and 95% CL bands, and observed upper limits, on $\tan\beta$ as a function of m_A for the $m_h^{\text{mod}+}$ (upper) and the hMSSM (lower) scenarios of the MSSM. The observed exclusion contour is indicated by the purple region, while the area under the red curve is excluded by requiring the neutral h boson mass consistent with 125 ± 3 GeV.

pected background due to standard model (SM) processes. The 95% confidence level upper limit for the production of beyond SM neutral Higgs bosons is determined in the framework of the $m_h^{\text{mod}+}$ and the phenomenological scenarios of the MSSM. For the ratio of the vacuum expectation values of the neutral components of the two Higgs doublets, $\tan\beta$, its excluded values range from ≈ 10 to ≈ 60 for a mass of the pseudoscalar A boson (m_A) from 130 to 600 GeV. The larger collected luminosity and the higher center-of-mass energy exclude a larger m_A - $\tan\beta$ region, compared to what was obtained at 7 and 8 TeV in a similar analysis. Model-independent exclusion limits on the production cross section times branching fraction of a generic narrow-width neutral boson decaying to two

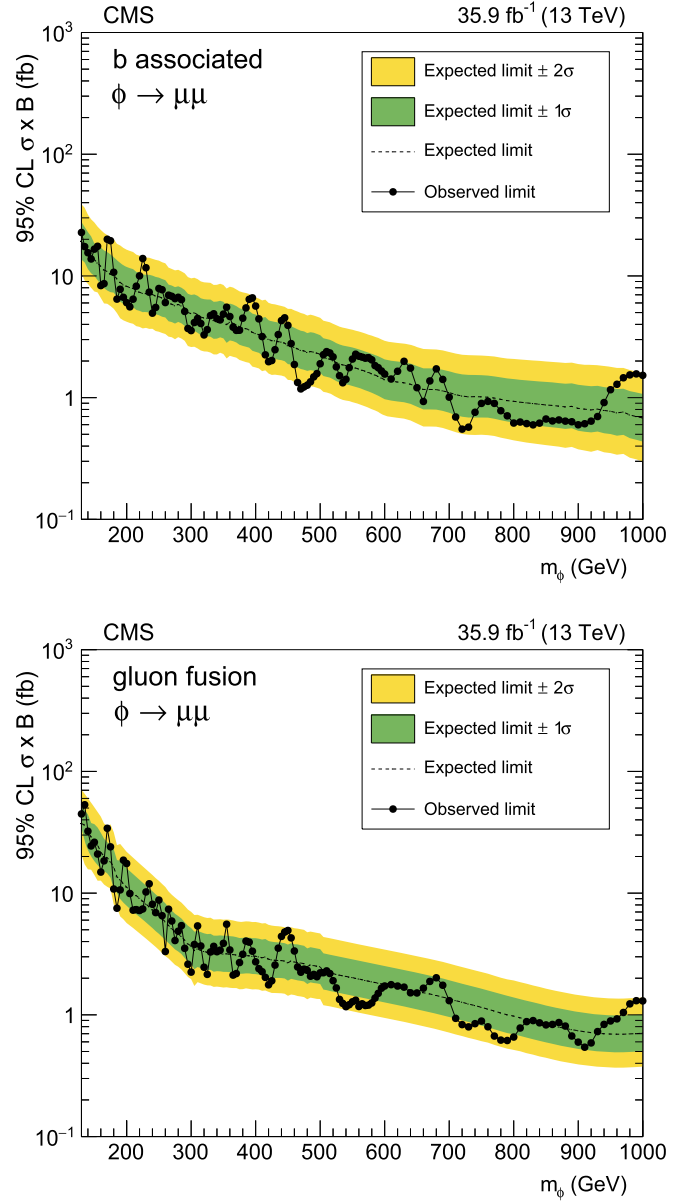


Fig. 6. The 95% CL expected, including the 68 and 95% CL bands, and observed model-independent upper limits on the production cross section times branching fraction of a generic ϕ boson decaying to a dimuon pair, in the case of b-associated (upper) and gluon fusion (lower) production. The results are obtained using a signal template with an intrinsic narrow width.

muons have been determined assuming the neutral boson to be produced entirely either via b-associated or gluon fusion mechanisms. The limits are determined in the mass range from 130 to 1000 GeV, separately for the two production mechanisms. Similarly, exclusion limits are also obtained assuming a signal width equal to 10% of its mass value.

Acknowledgements

We congratulate our colleagues in the CERN accelerator departments for the excellent performance of the LHC and thank the technical and administrative staffs at CERN and at other CMS institutes for their contributions to the success of the CMS effort. In addition, we gratefully acknowledge the computing centers and personnel of the Worldwide LHC Computing Grid for delivering so effectively the computing infrastructure essential to our analyses.

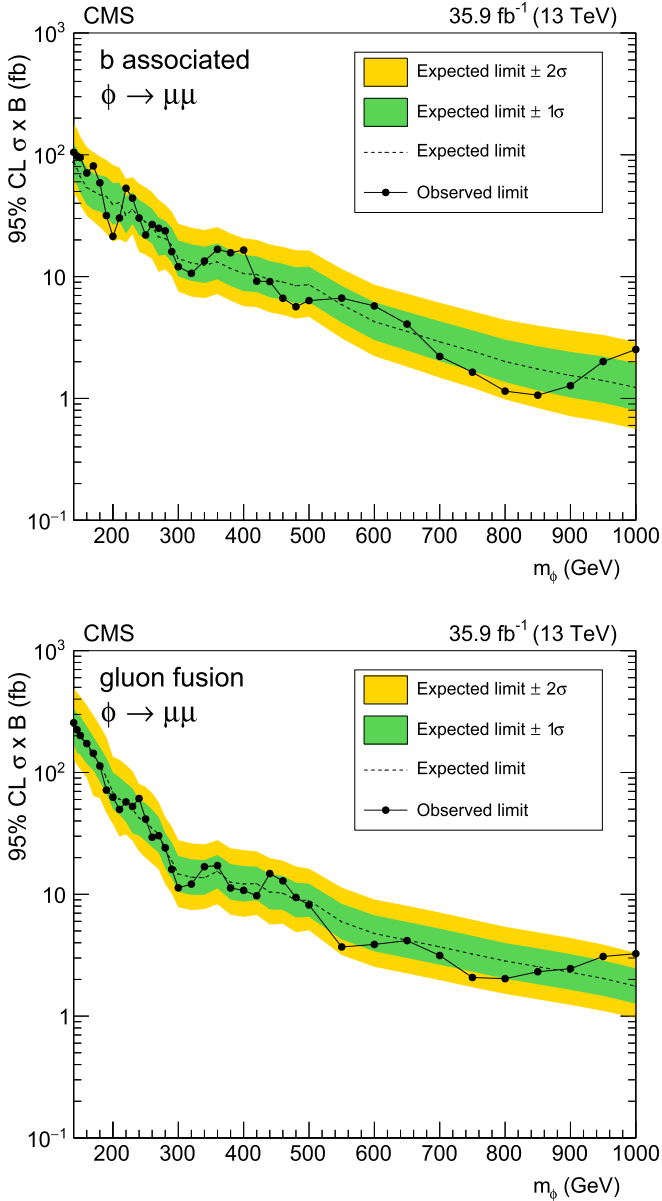


Fig. 7. The 95% CL expected, including the 68 and 95% CL bands, and observed model-independent upper limits on the production cross section times branching fraction of a generic ϕ boson decaying to a dimuon pair, in the case of b-associated (upper) and gluon fusion (lower) production. The results are obtained using a signal template with an intrinsic width equal to the 10% of the nominal mass.

Finally, we acknowledge the enduring support for the construction and operation of the LHC and the CMS detector provided by the following funding agencies: BMFWF and FWF (Austria); FNRS and FWO (Belgium); CNPq, CAPES, FAPERJ, and FAPESP (Brazil); MES (Bulgaria); CERN; CAS, MOST, and NSFC (China); COLCIENCIAS (Colombia); MSES and CSF (Croatia); RPF (Cyprus); SENESCYT (Ecuador); MoER, ERC IUT, and ERDF (Estonia); Academy of Finland, MEC, and HIP (Finland); CEA and CNRS/IN2P3 (France); BMBF, DFG, and HGF (Germany); GSRT (Greece); NKFI (Hungary); DAE and DST (India); IPM (Iran); SFI (Ireland); INFN (Italy); MSIP and NRF (Republic of Korea); LAS (Lithuania); MOE and UM (Malaysia); BUAP, CINVESTAV, CONACYT, LNS, SEP, and UASLP-FAI (Mexico); MBIE (New Zealand); PAEC (Pakistan); MSHE and NSC (Poland); FCT (Portugal); JINR (Dubna); MON, ROSATOM, RAS and RFBR (Russia); MESTD (Serbia); SEIDI, CPAN, PCTI and FEDER (Spain); Swiss Funding Agencies (Switzerland); MST (Taipei); ThEPCenter, IPST,

STAR, and NSTDA (Thailand); TUBITAK and TAEK (Turkey); NASU and SFFR (Ukraine); STFC (United Kingdom); DOE and NSF (USA).

Individuals have received support from the Marie-Curie program and the European Research Council and Horizon 2020 Grant, contract No. 675440 (European Union); the Leventis Foundation; the Alfred P. Sloan Foundation; the Alexander von Humboldt Foundation; the Belgian Federal Science Policy Office; the Fonds pour la Formation à la Recherche dans l'Industrie et dans l'Agriculture (FRIA-Belgium); the Agentschap voor Innovatie door Wetenschap en Technologie (IWT-Belgium); the F.R.S.-FNRS and FWO (Belgium) under the "Excellence of Science - EOS" - be.h project n. 30820817; the Ministry of Education, Youth and Sports (MEYS) of the Czech Republic; the Lendület ("Momentum") Program and the János Bolyai Research Scholarship of the Hungarian Academy of Sciences, the New National Excellence Program ÚNKP, the NKFI research grants 123842, 123959, 124845, 124850 and 125105 (Hungary); the Council of Science and Industrial Research, India; the HOMING PLUS program of the Foundation for Polish Science, cofinanced from European Union, Regional Development Fund, the Mobility Plus program of the Ministry of Science and Higher Education, the National Science Center (Poland), contracts Harmonia 2014/14/M/ST2/00428, Opus 2014/13/B/ST2/02543, 2014/15/B/ST2/03998, and 2015/19/B/ST2/02861, Sonata-bis 2012/07/E/ST2/01406; the National Priorities Research Program by Qatar National Research Fund; the Programa Estatal de Fomento de la Investigación Científica y Técnica de Excelencia María de Maeztu, grant MDM-2015-0509 and the Programa Severo Ochoa del Principado de Asturias; the Thalís and Aristeia programs cofinanced by EU-ESF and the Greek NSRF; the Rachadapisek Sompot Fund for Postdoctoral Fellowship, Chulalongkorn University and the Chulalongkorn Academic into Its 2nd Century Project Advancement Project (Thailand); The Welch Foundation, contract C-1845; and the Weston Havens Foundation (USA).

References

- [1] ATLAS Collaboration, Observation of a new particle in the search for the standard model Higgs boson with the ATLAS detector at the LHC, Phys. Lett. B 716 (2012) 1, <https://doi.org/10.1016/j.physletb.2012.08.020>, arXiv:1207.7214.
- [2] CMS Collaboration, Observation of a new boson at a mass of 125 GeV with the CMS experiment at the LHC, Phys. Lett. B 716 (2012) 30, <https://doi.org/10.1016/j.physletb.2012.08.021>, arXiv:1207.7235.
- [3] CMS Collaboration, Observation of a new boson with mass near 125 GeV in pp collisions at $\sqrt{s} = 7$ and 8 TeV, J. High Energy Phys. 06 (2013) 081, [https://doi.org/10.1007/JHEP06\(2013\)081](https://doi.org/10.1007/JHEP06(2013)081), arXiv:1303.4571.
- [4] ATLAS Collaboration, CMS Collaboration, Combined measurement of the Higgs boson mass in pp collisions at $\sqrt{s} = 7$ and 8 TeV with the ATLAS and CMS experiments, Phys. Rev. Lett. 114 (2015) 191803, <https://doi.org/10.1103/PhysRevLett.114.191803>, arXiv:1503.07589.
- [5] ATLAS Collaboration, CMS Collaborations, Measurements of the Higgs boson production and decay rates and constraints on its couplings from a combined ATLAS and CMS analysis of the LHC pp collision data at $\sqrt{s} = 7$ and 8 TeV, J. High Energy Phys. 08 (2016) 045, [https://doi.org/10.1007/JHEP08\(2016\)045](https://doi.org/10.1007/JHEP08(2016)045), arXiv:1606.02266.
- [6] Yu.A. Golfand, E.P. Likhtman, Extension of the algebra of Poincaré group generators and violation of p invariance, JETP Lett. 13 (1971) 323, URL: http://www.jetpletters.ac.ru/ps/1584/article_24309.pdf.
- [7] J. Wess, B. Zumino, Supergauge transformations in four-dimensions, Nucl. Phys. B 70 (1974) 39, [https://doi.org/10.1016/0550-3213\(74\)90355-1](https://doi.org/10.1016/0550-3213(74)90355-1).
- [8] P. Fayet, Supergauge invariant extension of the Higgs mechanism and a model for the electron and its neutrino, Nucl. Phys. B 90 (1975) 104, [https://doi.org/10.1016/0550-3213\(75\)90636-7](https://doi.org/10.1016/0550-3213(75)90636-7).
- [9] P. Fayet, Spontaneously broken supersymmetric theories of weak, electromagnetic and strong interactions, Phys. Lett. B 69 (1977) 489, [https://doi.org/10.1016/0370-2693\(77\)90852-8](https://doi.org/10.1016/0370-2693(77)90852-8).
- [10] A. Djouadi, The anatomy of electroweak symmetry breaking. II. The Higgs bosons in the minimal supersymmetric model, Phys. Rep. 459 (2008) 1, <https://doi.org/10.1016/j.physrep.2007.10.005>, arXiv:hep-ph/0503173.
- [11] M. Carena, S. Heinemeyer, O. Stål, C.E.M. Wagner, G. Weiglein, MSSM Higgs boson searches at the LHC: benchmark scenarios after the discovery of a Higgs-like particle, Eur. Phys. J. C 73 (2013) 2552, <https://doi.org/10.1140/epjc/s10052-013-2552-1>, arXiv:1302.7033.

- [12] P. Bechtel, S. Heinemeyer, O. Stål, T. Stefaniak, G. Weiglein, Probing the standard model with Higgs signal rates from the Tevatron, the LHC and a future ILC, *J. High Energy Phys.* 11 (2014) 039, [https://doi.org/10.1007/JHEP11\(2014\)039](https://doi.org/10.1007/JHEP11(2014)039), arXiv:1403.1582.
- [13] L. Maiani, A.D. Polosa, V. Riquer, Bounds to the Higgs sector masses in minimal supersymmetry from LHC data, *Phys. Lett. B* 724 (2013) 274, <https://doi.org/10.1016/j.physletb.2013.06.026>, arXiv:1305.2172.
- [14] A. Djouadi, L. Maiani, G. Moreau, A. Polosa, J. Quevillon, V. Riquer, The post-Higgs MSSM scenario: Habemus MSSM?, *Eur. Phys. J. C* 73 (2013) 2650, <https://doi.org/10.1140/epjc/s10052-013-2650-0>, arXiv:1307.5205.
- [15] A. Djouadi, L. Maiani, A. Polosa, J. Quevillon, V. Riquer, Fully covering the MSSM Higgs sector at the LHC, *J. High Energy Phys.* 06 (2015) 168, [https://doi.org/10.1007/JHEP06\(2015\)168](https://doi.org/10.1007/JHEP06(2015)168), arXiv:1502.05653.
- [16] A. Djouadi, J. Quevillon, The MSSM Higgs sector at a high M_{SUSY} : reopening the low $\tan\beta$ regime and heavy Higgs searches, *J. High Energy Phys.* 10 (2013) 028, [https://doi.org/10.1007/JHEP10\(2013\)028](https://doi.org/10.1007/JHEP10(2013)028), arXiv:1304.1787.
- [17] E. Bagnaschi, et al., MSSM Higgs boson searches at the LHC: benchmark scenarios for Run 2 and beyond, *Eur. Phys. J. C* 79 (2019) 617, <https://doi.org/10.1140/epjc/s10052-019-7114-8>, arXiv:1808.07542.
- [18] CMS Collaboration, Measurements of the Higgs boson width and anomalous HVV couplings from on-shell and off-shell production in the four-lepton final state, *Phys. Rev. D* 99 (2019) 112003, <https://doi.org/10.1103/PhysRevD.99.112003>, arXiv:1901.00174.
- [19] ATLAS Collaboration, Constraints on off-shell Higgs boson production and the Higgs boson total width in $ZZ \rightarrow 4\ell$ and $ZZ \rightarrow 2\ell 2\nu$ final states with the ATLAS detector, *Phys. Lett. B* 786 (2018) 223, <https://doi.org/10.1016/j.physletb.2018.09.048>, arXiv:1808.01191.
- [20] ATLAS Collaboration, Search for the neutral Higgs bosons of the minimal supersymmetric standard model in pp collisions at $\sqrt{s} = 7$ TeV with the ATLAS detector, *J. High Energy Phys.* 02 (2013) 095, [https://doi.org/10.1007/JHEP02\(2013\)095](https://doi.org/10.1007/JHEP02(2013)095), arXiv:1211.6956.
- [21] CMS Collaboration, Search for neutral MSSM Higgs bosons decaying to $\mu^+\mu^-$ in pp collisions at $\sqrt{s} = 7$ and 8 TeV, *Phys. Lett. B* 752 (2016) 221, <https://doi.org/10.1016/j.physletb.2015.11.042>, arXiv:1508.01437.
- [22] ATLAS Collaboration, Search for scalar resonances decaying into $\mu^+\mu^-$ in events with and without b-tagged jets produced in proton-proton collisions at $\sqrt{s} = 13$ TeV with the ATLAS detector, *J. High Energy Phys.* 07 (2019) 117, [https://doi.org/10.1007/JHEP07\(2019\)117](https://doi.org/10.1007/JHEP07(2019)117), arXiv:1901.08144.
- [23] ATLAS Collaboration, Search for neutral Higgs bosons of the minimal supersymmetric standard model in pp collisions at $\sqrt{s} = 8$ TeV with the ATLAS detector, *J. High Energy Phys.* 11 (2014) 056, [https://doi.org/10.1007/JHEP11\(2014\)056](https://doi.org/10.1007/JHEP11(2014)056), arXiv:1409.6064.
- [24] ATLAS Collaboration, Search for minimal supersymmetric standard model Higgs bosons H/A and for a Z' boson in the $\tau\tau$ final state produced in pp collisions at $\sqrt{s} = 13$ TeV with the ATLAS detector, *Eur. Phys. J. C* 76 (2016) 585, <https://doi.org/10.1140/epjc/s10052-016-4400-6>, arXiv:1608.00890.
- [25] ATLAS Collaboration, Search for additional heavy neutral Higgs and gauge bosons in the ditau final state produced in 36 fb $^{-1}$ of pp collisions at $\sqrt{s} = 13$ TeV with the ATLAS detector, *J. High Energy Phys.* 01 (2018) 055, [https://doi.org/10.1007/JHEP01\(2018\)055](https://doi.org/10.1007/JHEP01(2018)055), arXiv:1709.07242.
- [26] CMS Collaboration, Search for neutral minimal supersymmetric standard model Higgs bosons decaying to tau pairs in pp collisions at $\sqrt{s} = 7$ TeV, *Phys. Rev. Lett.* 106 (2011) 231801, <https://doi.org/10.1103/PhysRevLett.106.231801>, arXiv:1104.1619.
- [27] CMS Collaboration, Search for neutral Higgs bosons decaying to tau pairs in pp collisions at $\sqrt{s} = 7$ TeV, *Phys. Lett. B* 713 (2012) 68, <https://doi.org/10.1016/j.physletb.2012.05.028>, arXiv:1202.4083.
- [28] CMS Collaboration, Search for additional neutral MSSM Higgs bosons in the $\tau\tau$ final state in proton-proton collisions at $\sqrt{s} = 13$ TeV, *J. High Energy Phys.* 08 (2018) 007, [https://doi.org/10.1007/JHEP08\(2018\)007](https://doi.org/10.1007/JHEP08(2018)007), arXiv:1803.06553.
- [29] CMS Collaboration, Search for a Higgs boson decaying into a b-quark pair and produced in association with b quarks in proton-proton collisions at 7 TeV, *Phys. Lett. B* 722 (2013) 207, <https://doi.org/10.1016/j.physletb.2013.04.017>, arXiv:1302.2892.
- [30] CMS Collaboration, Search for neutral MSSM Higgs bosons decaying into a pair of bottom quarks, *J. High Energy Phys.* 11 (2015) 071, [https://doi.org/10.1007/JHEP11\(2015\)071](https://doi.org/10.1007/JHEP11(2015)071), arXiv:1506.08329.
- [31] CMS Collaboration, Search for beyond the standard model Higgs bosons decaying into a $b\bar{b}$ pair in pp collisions at $\sqrt{s} = 13$ TeV, *J. High Energy Phys.* 08 (2018) 113, [https://doi.org/10.1007/JHEP08\(2018\)113](https://doi.org/10.1007/JHEP08(2018)113), arXiv:1805.12191.
- [32] The LEP Collaborations: ALEPH, DELPHI, L3, and OPAL, and the LEP Working Group for Higgs Boson Searches, Search for neutral MSSM Higgs bosons at LEP, *Eur. Phys. J. C* 47 (2006) 547, <https://doi.org/10.1140/epjc/s2006-02569-7>, arXiv:hep-ex/0602042.
- [33] T. Aaltonen, et al., CDF, Search for Higgs bosons predicted in two-Higgs-doublet models via decays to tau lepton pairs in 1.96 TeV $p\bar{p}$ collisions, *Phys. Rev. Lett.* 103 (2009) 201801, <https://doi.org/10.1103/PhysRevLett.103.201801>, arXiv:0906.1014.
- [34] T. Aaltonen, et al., CDF, Search for Higgs bosons produced in association with b-quarks, *Phys. Rev. D* 85 (2012) 032005, <https://doi.org/10.1103/PhysRevD.85.032005>, arXiv:1106.4782.
- [35] V.M. Abazov, et al., D0, Search for neutral Higgs bosons in the multi-b-jet topology in 5.2 fb $^{-1}$ of $p\bar{p}$ collisions at $\sqrt{s} = 1.96$ TeV, *Phys. Lett. B* 698 (2011) 97, <https://doi.org/10.1016/j.physletb.2011.02.062>, arXiv:1011.1931.
- [36] V.M. Abazov, et al., D0, Search for Higgs bosons decaying to $\tau\tau$ pairs in $p\bar{p}$ collisions at $\sqrt{s} = 1.96$ TeV, *Phys. Lett. B* 707 (2012) 323, <https://doi.org/10.1016/j.physletb.2011.12.050>, arXiv:1106.4555.
- [37] CMS Collaboration, The CMS experiment at the CERN LHC, *J. Instrum.* 3 (2008) S08004, <https://doi.org/10.1088/1748-0221/3/08/S08004>.
- [38] T. Sjöstrand, S. Ask, J.R. Christiansen, R. Corke, N. Desai, P. Ilten, S. Mrenna, S. Prestel, C.O. Rasmussen, P.Z. Skands, An introduction to PYTHIA 8.2, *Comput. Phys. Commun.* 191 (2015) 159, <https://doi.org/10.1016/j.cpc.2015.01.024>, arXiv:1410.3012.
- [39] P. Nason, A new method for combining NLO QCD with shower Monte Carlo algorithms, *J. High Energy Phys.* 11 (2004) 040, <https://doi.org/10.1088/1126-6708/2004/11/040>, arXiv:hep-ph/0409146.
- [40] J. Alwall, R. Frederix, S. Frixione, V. Hirschi, F. Maltoni, O. Mattelaer, H.S. Shao, T. Stelzer, P. Torrielli, M. Zaro, The automated computation of tree-level and next-to-leading order differential cross sections, and their matching to parton shower simulations, *J. High Energy Phys.* 07 (2014) 079, [https://doi.org/10.1007/JHEP07\(2014\)079](https://doi.org/10.1007/JHEP07(2014)079), arXiv:1405.0301.
- [41] P. Artoisenet, R. Frederix, O. Mattelaer, R. Rietkerk, Automatic spin-entangled decays of heavy resonances in Monte Carlo simulations, *J. High Energy Phys.* 03 (2013) 015, [https://doi.org/10.1007/JHEP03\(2013\)015](https://doi.org/10.1007/JHEP03(2013)015), arXiv:1212.3460.
- [42] R.D. Ball, V. Bertone, F. Cerutti, L. Del Debbio, S. Forte, A. Guffanti, J.I. Latorre, J. Rojo, M. Ubiali, NNPDF, Unbiased global determination of parton distributions and their uncertainties at NNLO and at LO, *Nucl. Phys. B* 855 (2012) 153, <https://doi.org/10.1016/j.nuclphysb.2011.09.024>, arXiv:1107.2652.
- [43] CMS Collaboration, Event generator tunes obtained from underlying event and multiparton scattering measurements, *Eur. Phys. J. C* 76 (2016) 155, <https://doi.org/10.1140/epjc/s10052-016-3988-x>, arXiv:1512.00815.
- [44] S. Agostinelli, et al., GEANT4, GEANT4—a simulation toolkit, *Nucl. Instrum. Methods A* 506 (2003) 250, [https://doi.org/10.1016/S0168-9002\(03\)01368-8](https://doi.org/10.1016/S0168-9002(03)01368-8).
- [45] D. de Florian, et al., Handbook of LHC Higgs Cross Sections: 4. Deciphering the Nature of the Higgs Sector, CERN Report CERN-2017-002-M, 2016, <https://doi.org/10.23731/CYRM-2017-002>, arXiv:1610.07922.
- [46] J.R. Andersen, et al., Handbook of LHC Higgs Cross Sections: 3. Higgs Properties, CERN Report CERN-2013-004, 2013, <https://doi.org/10.5170/CERN-2013-004>, arXiv:1307.1347.
- [47] S. Heinemeyer, W. Hollik, G. Weiglein, FeynHiggs: a program for the calculation of the masses of the neutral CP-even Higgs bosons in the MSSM, *Comput. Phys. Commun.* 124 (2000) 76, [https://doi.org/10.1016/S0010-4655\(99\)00364-1](https://doi.org/10.1016/S0010-4655(99)00364-1), arXiv:hep-ph/9812320.
- [48] S. Heinemeyer, W. Hollik, G. Weiglein, The masses of the neutral CP-even Higgs bosons in the MSSM: accurate analysis at the two-loop level, *Eur. Phys. J. C* 9 (1999) 343, <https://doi.org/10.1007/s100529900006>, arXiv:hep-ph/9812472.
- [49] G. Degrandi, S. Heinemeyer, W. Hollik, P. Slavich, G. Weiglein, Towards high-precision predictions for the MSSM Higgs sector, *Eur. Phys. J. C* 28 (2003) 133, <https://doi.org/10.1140/epjc/s2003-01152-2>, arXiv:hep-ph/0212020.
- [50] M. Frank, T. Hahn, S. Heinemeyer, W. Hollik, H. Rzehak, G. Weiglein, The Higgs boson masses and mixings of the complex MSSM in the Feynman-diagrammatic approach, *J. High Energy Phys.* 02 (2007) 047, <https://doi.org/10.1088/1126-6708/2007/02/047>, arXiv:hep-ph/0611326.
- [51] T. Hahn, S. Heinemeyer, W. Hollik, H. Rzehak, G. Weiglein, High-precision predictions for the light CP-even Higgs boson mass of the minimal supersymmetric standard model, *Phys. Rev. Lett.* 112 (2014) 141801, <https://doi.org/10.1103/PhysRevLett.112.141801>, arXiv:1312.4937.
- [52] R.V. Harlander, S. Liebler, H. Mantler, SusHi: a program for the calculation of Higgs production in gluon fusion and bottom-quark annihilation in the standard model and the MSSM, *Comput. Phys. Commun.* 184 (2013) 1605, <https://doi.org/10.1016/j.cpc.2013.02.006>, arXiv:1212.3249.
- [53] M. Spira, A. Djouadi, D. Graudenz, P.M. Zerwas, Higgs boson production at the LHC, *Nucl. Phys. B* 453 (1995) 17, [https://doi.org/10.1016/0550-3213\(95\)00379-7](https://doi.org/10.1016/0550-3213(95)00379-7), arXiv:hep-ph/9504378.
- [54] R.V. Harlander, M. Steinhauser, Supersymmetric Higgs production in gluon fusion at next-to-leading order, *J. High Energy Phys.* 09 (2004) 066, <https://doi.org/10.1088/1126-6708/2004/09/066>, arXiv:hep-ph/0409010.
- [55] R. Harlander, P. Kant, Higgs production and decay: analytic results at next-to-leading order QCD, *J. High Energy Phys.* 12 (2005) 015, <https://doi.org/10.1088/1126-6708/2005/12/015>, arXiv:hep-ph/0509189.
- [56] G. Degrandi, P. Slavich, NLO QCD bottom corrections to Higgs boson production in the MSSM, *J. High Energy Phys.* 11 (2010) 044, [https://doi.org/10.1007/JHEP11\(2010\)044](https://doi.org/10.1007/JHEP11(2010)044), arXiv:1007.3465.
- [57] G. Degrandi, S. Di Vita, P. Slavich, NLO QCD corrections to pseudoscalar Higgs production in the MSSM, *J. High Energy Phys.* 08 (2011) 128, [https://doi.org/10.1007/JHEP08\(2011\)128](https://doi.org/10.1007/JHEP08(2011)128), arXiv:1107.0914.

- [58] G. Degrandi, S. Di Vita, P. Slavich, On the NLO QCD corrections to the production of the heaviest neutral Higgs scalar in the MSSM, *Eur. Phys. J. C* 72 (2012) 2032, <https://doi.org/10.1140/epjc/s10052-012-2032-z>, arXiv:1204.1016.
- [59] R.V. Harlander, W.B. Kilgore, Next-to-next-to-leading order Higgs production at hadron colliders, *Phys. Rev. Lett.* 88 (2002) 201801, <https://doi.org/10.1103/PhysRevLett.88.201801>, arXiv:hep-ph/0201206.
- [60] C. Anastasiou, K. Melnikov, Higgs boson production at hadron colliders in NNLO QCD, *Nucl. Phys. B* 646 (2002) 220, [https://doi.org/10.1016/S0550-3213\(02\)00837-4](https://doi.org/10.1016/S0550-3213(02)00837-4), arXiv:hep-ph/0207004.
- [61] V. Ravindran, J. Smith, W.L. van Neerven, NNLO corrections to the total cross-section for Higgs boson production in hadron-hadron collisions, *Nucl. Phys. B* 665 (2003) 325, [https://doi.org/10.1016/S0550-3213\(03\)00457-7](https://doi.org/10.1016/S0550-3213(03)00457-7), arXiv:hep-ph/0302135.
- [62] R.V. Harlander, W.B. Kilgore, Production of a pseudo-scalar Higgs boson at hadron colliders at next-to-next-to leading order, *J. High Energy Phys.* 10 (2002) 017, <https://doi.org/10.1088/1126-6708/2002/10/017>, arXiv:hep-ph/0208096.
- [63] C. Anastasiou, K. Melnikov, Pseudoscalar Higgs boson production at hadron colliders in next-to-next-to-leading order QCD, *Phys. Rev. D* 67 (2003) 037501, <https://doi.org/10.1103/PhysRevD.67.037501>, arXiv:hep-ph/0208115.
- [64] U. Aglietti, R. Bonciani, G. Degrandi, A. Vicini, Two-loop light fermion contribution to Higgs production and decays, *Phys. Lett. B* 595 (2004) 432, <https://doi.org/10.1016/j.physletb.2004.06.063>, arXiv:hep-ph/0404071.
- [65] R. Bonciani, G. Degrandi, A. Vicini, On the generalized harmonic polylogarithms of one complex variable, *Comput. Phys. Commun.* 182 (2011) 1253, <https://doi.org/10.1016/j.cpc.2011.02.011>, arXiv:1007.1891.
- [66] R. Harlander, M. Kramer, M. Schumacher, Bottom-quark associated Higgs-boson production: reconciling the four- and five-flavour scheme approach, arXiv:1112.3478, 2011.
- [67] R.V. Harlander, W.B. Kilgore, Higgs boson production in bottom quark fusion at next-to-next-to leading order, *Phys. Rev. D* 68 (2003) 013001, <https://doi.org/10.1103/PhysRevD.68.013001>, arXiv:hep-ph/0304035.
- [68] S. Dittmaier, M. Krämer, M. Spira, Higgs radiation off bottom quarks at the Fermilab Tevatron and the CERN LHC, *Phys. Rev. D* 70 (2004) 074010, <https://doi.org/10.1103/PhysRevD.70.074010>, arXiv:hep-ph/0309204.
- [69] S. Dawson, C.B. Jackson, L. Reina, D. Wackerroth, Exclusive Higgs boson production with bottom quarks at hadron colliders, *Phys. Rev. D* 69 (2004) 074027, <https://doi.org/10.1103/PhysRevD.69.074027>, arXiv:hep-ph/0311067.
- [70] A. Djouadi, J. Kalinowski, M. Spira, HDECAY: a program for Higgs boson decays in the standard model and its supersymmetric extension, *Comput. Phys. Commun.* 108 (1998) 56, [https://doi.org/10.1016/S0010-4655\(97\)00123-9](https://doi.org/10.1016/S0010-4655(97)00123-9), arXiv:hep-ph/9704448.
- [71] M. Czakon, A. Mitov, Top++: a program for the calculation of the top-pair cross-section at hadron colliders, *Comput. Phys. Commun.* 185 (2014) 2930, <https://doi.org/10.1016/j.cpc.2014.06.021>, arXiv:1112.5675.
- [72] R. Gavin, Y. Li, F. Petriello, S. Quackenbush, FEWZ 2.0: a code for hadronic Z production at next-to-next-to-leading order, *Comput. Phys. Commun.* 182 (2011) 2388, <https://doi.org/10.1016/j.cpc.2011.06.008>, arXiv:1011.3540.
- [73] M. Aliev, H. Lacker, U. Langenfeld, S. Moch, P. Uwer, M. Wiedermann, HATHOR: HAdronic Top and Heavy quarks crOss section calculator, *Comput. Phys. Commun.* 182 (2011) 1034, <https://doi.org/10.1016/j.cpc.2010.12.040>, arXiv:1007.1327.
- [74] P. Kant, O.M. Kind, T. Kintscher, T. Lohse, T. Martini, S. Mölbitz, P. Rieck, P. Uwer, HatHor for single top-quark production: updated predictions and uncertainty estimates for single top-quark production in hadronic collisions, *Comput. Phys. Commun.* 191 (2015) 74, <https://doi.org/10.1016/j.cpc.2015.02.001>, arXiv:1406.4403.
- [75] J.M. Campbell, R.K. Ellis, C. Williams, Vector boson pair production at the LHC, *J. High Energy Phys.* 11 (2011) 018, [https://doi.org/10.1007/JHEP07\(2011\)018](https://doi.org/10.1007/JHEP07(2011)018), arXiv:1105.0020.
- [76] CMS Collaboration, Particle-flow reconstruction and global event description with the CMS detector, *J. Instrum.* 12 (2017) P10003, <https://doi.org/10.1088/1748-0221/12/10/P10003>, arXiv:1706.04965.
- [77] CMS Collaboration, Performance of CMS muon reconstruction in pp collision events at $\sqrt{s} = 7$ TeV, *J. Instrum.* 7 (2012) P10002, <https://doi.org/10.1088/1748-0221/7/10/P10002>, arXiv:1206.4071.
- [78] CMS Collaboration, Performance of the CMS muon detector and muon reconstruction with proton-proton collisions at $\sqrt{s} = 13$ TeV, *J. Instrum.* 13 (2018) P06015, <https://doi.org/10.1088/1748-0221/13/06/P06015>, arXiv:1804.04528.
- [79] M. Cacciari, G.P. Salam, G. Soyez, The anti- k_T jet clustering algorithm, *J. High Energy Phys.* 04 (2008) 063, <https://doi.org/10.1088/1126-6708/2008/04/063>, arXiv:0802.1189.
- [80] M. Cacciari, G.P. Salam, G. Soyez, FastJet user manual, *Eur. Phys. J. C* 72 (2012) 1896, <https://doi.org/10.1140/epjc/s10052-012-1896-2>, arXiv:1111.6097.
- [81] K. Rose, Deterministic annealing for clustering, compression, classification, regression, and related optimization problems, *IEEE Proc.* 86 (1998) 2210, <https://doi.org/10.1109/5.726788>.
- [82] CMS Collaboration, Identification of heavy-flavour jets with the CMS detector in pp collisions at 13 TeV, *J. Instrum.* 13 (2018) P05011, <https://doi.org/10.1088/1748-0221/13/05/P05011>, arXiv:1712.07158.
- [83] CMS Collaboration, The CMS trigger system, *J. Instrum.* 12 (2017) P01020, <https://doi.org/10.1088/1748-0221/12/01/P01020>, arXiv:1609.02366.
- [84] M. Cacciari, G.P. Salam, Pileup subtraction using jet areas, *Phys. Lett. B* 659 (2008) 119, <https://doi.org/10.1016/j.physletb.2007.09.077>, arXiv:0707.1378.
- [85] CMS Collaboration, Measurement of the inelastic proton-proton cross section at $\sqrt{s} = 13$ TeV, *J. High Energy Phys.* 07 (2018) 161, [https://doi.org/10.1007/JHEP07\(2018\)161](https://doi.org/10.1007/JHEP07(2018)161), arXiv:1802.02613.
- [86] ATLAS Collaboration, Measurement of the inelastic proton-proton cross section at $\sqrt{s} = 13$ TeV with the ATLAS detector at the LHC, *Phys. Rev. Lett.* 117 (2016) 182002, <https://doi.org/10.1103/PhysRevLett.117.182002>, arXiv:1606.02625.
- [87] CMS Collaboration, Determination of jet energy calibration and transverse momentum resolution in CMS, *J. Instrum.* 6 (2011) P11002, <https://doi.org/10.1088/1748-0221/6/11/P11002>, arXiv:1107.4277.
- [88] CMS Collaboration, CMS Luminosity Measurements for the 2016 Data Taking Period, CMS Physics Analysis Summary CMS-PAS-LUM-17-001, URL: <http://cds.cern.ch/record/2257069>.
- [89] CMS Collaboration, Search for the Higgs boson decaying to two muons in proton-proton collisions at $\sqrt{s} = 13$ TeV, *Phys. Rev. Lett.* 122 (2019) 021801, <https://doi.org/10.1103/PhysRevLett.122.021801>, arXiv:1807.06325.
- [90] T. Junk, Confidence level computation for combining searches with small statistics, *Nucl. Instrum. Methods A* 434 (1999) 435, [https://doi.org/10.1016/S0168-9002\(99\)00498-2](https://doi.org/10.1016/S0168-9002(99)00498-2), arXiv:hep-ex/9902006.
- [91] A.L. Read, Presentation of search results: the CL_s technique, *J. Phys. G* 28 (2002) 2693, <https://doi.org/10.1088/0954-3899/28/10/313>.
- [92] The ATLAS Collaboration, The CMS Collaboration, The LHC Higgs Combination Group, Procedure for the LHC Higgs Boson Search Combination in Summer 2011, Technical Report CMS-NOTE-2011-005, ATL-PHYS-PUB-2011-11, 2011, URL: <https://cds.cern.ch/record/1379837>.

The CMS Collaboration

A.M. Sirunyan[†], A. Tumasyan

Yerevan Physics Institute, Yerevan, Armenia

W. Adam, F. Ambrogio, T. Bergauer, J. Brandstetter, M. Dragicevic, J. Erö, A. Escalante Del Valle, M. Flechl, R. Frühwirth¹, M. Jeitler¹, N. Krammer, I. Krätschmer, D. Liko, T. Madlener, I. Mikulec, N. Rad, J. Schieck¹, R. Schöfbeck, M. Spanring, D. Spitzbart, W. Waltenberger, J. Wittmann, C.-E. Wulz¹, M. Zarucki

Institut für Hochenergiephysik, Wien, Austria

V. Drugakov, V. Mossolov, J. Suarez Gonzalez

Institute for Nuclear Problems, Minsk, Belarus

M.R. Darwish, E.A. De Wolf, D. Di Croce, X. Janssen, J. Lauwers, A. Lelek, M. Pieters, H. Van Haevermaet, P. Van Mechelen, N. Van Remortel

Universiteit Antwerpen, Antwerpen, Belgium

F. Blekman, J. D'Hondt, J. De Clercq, G. Flouris, D. Lontkovskyi, S. Lowette, I. Marchesini, S. Moortgat, L. Moreels, Q. Python, K. Skovpen, S. Tavernier, W. Van Doninck, P. Van Mulders, I. Van Parijs

Vrije Universiteit Brussel, Brussel, Belgium

D. Beghin, B. Bilin, H. Brun, B. Clerbaux, G. De Lentdecker, H. Delannoy, B. Dorney, L. Favart, A. Grebenyuk, A.K. Kalsi, J. Luetic, A. Popov, N. Postiau, E. Starling, L. Thomas, C. Vander Velde, P. Vanlaer, D. Vannerom, Q. Wang

Université Libre de Bruxelles, Bruxelles, Belgium

T. Cornelis, D. Dobur, A. Fagot, M. Gul, I. Khvastunov², C. Roskas, D. Trocino, M. Tytgat, W. Verbeke, B. Vermassen, M. Vit, N. Zaganidis

Ghent University, Ghent, Belgium

O. Bondu, G. Bruno, C. Caputo, P. David, C. Delaere, M. Delcourt, A. Giammanco, G. Krintiras, V. Lemaitre, A. Magitteri, K. Piotrkowski, A. Saggio, M. Vidal Marono, P. Vischia, J. Zobec

Université Catholique de Louvain, Louvain-la-Neuve, Belgium

F.L. Alves, G.A. Alves, G. Correia Silva, C. Hensel, A. Moraes, P. Rebello Teles

Centro Brasileiro de Pesquisas Físicas, Rio de Janeiro, Brazil

E. Belchior Batista Das Chagas, W. Carvalho, J. Chinellato³, E. Coelho, E.M. Da Costa, G.G. Da Silveira⁴, D. De Jesus Damiao, C. De Oliveira Martins, S. Fonseca De Souza, L.M. Huertas Guativa, H. Malbouisson, D. Matos Figueiredo, M. Medina Jaime⁵, M. Melo De Almeida, C. Mora Herrera, L. Mundim, H. Nogima, W.L. Prado Da Silva, L.J. Sanchez Rosas, A. Santoro, A. Sznajder, M. Thiel, E.J. Tonelli Manganote³, F. Torres Da Silva De Araujo, A. Vilela Pereira

Universidade do Estado do Rio de Janeiro, Rio de Janeiro, Brazil

S. Ahuja^a, C.A. Bernardes^a, L. Calligaris^a, D. De Souza Lemos, T.R. Fernandez Perez Tomei^a, E.M. Gregores^b, P.G. Mercadante^b, S.F. Novaes^a, Sandra S. Padula^a

^a *Universidade Estadual Paulista, São Paulo, Brazil*

^b *Universidade Federal do ABC, São Paulo, Brazil*

A. Aleksandrov, G. Antchev, R. Hadjiiska, P. Iaydjiev, A. Marinov, M. Misheva, M. Rodozov, M. Shopova, G. Sultanov

Institute for Nuclear Research and Nuclear Energy, Bulgarian Academy of Sciences, Sofia, Bulgaria

A. Dimitrov, L. Litov, B. Pavlov, P. Petkov

University of Sofia, Sofia, Bulgaria

W. Fang⁶, X. Gao⁶, L. Yuan

Beihang University, Beijing, China

M. Ahmad, G.M. Chen, H.S. Chen, M. Chen, C.H. Jiang, D. Leggat, H. Liao, Z. Liu, S.M. Shaheen⁷, A. Spiezia, J. Tao, E. Yazgan, H. Zhang, S. Zhang⁷, J. Zhao

Institute of High Energy Physics, Beijing, China

A. Agapitos, Y. Ban, G. Chen, A. Levin, J. Li, L. Li, Q. Li, Y. Mao, S.J. Qian, D. Wang

State Key Laboratory of Nuclear Physics and Technology, Peking University, Beijing, China

Y. Wang

Tsinghua University, Beijing, China

C. Avila, A. Cabrera, L.F. Chaparro Sierra, C. Florez, C.F. González Hernández, M.A. Segura Delgado

Universidad de Los Andes, Bogota, Colombia

J.D. Ruiz Alvarez

Universidad de Antioquia, Medellin, Colombia

D. Giljanović, N. Godinovic, D. Lelas, I. Puljak, T. Sculac

University of Split, Faculty of Electrical Engineering, Mechanical Engineering and Naval Architecture, Split, Croatia

Z. Antunovic, M. Kovac

University of Split, Faculty of Science, Split, Croatia

V. Brigljevic, D. Ferencek, K. Kadija, B. Mesic, M. Roguljic, A. Starodumov⁸, T. Susa

Institute Rudjer Boskovic, Zagreb, Croatia

M.W. Ather, A. Attikis, E. Erodotou, A. Ioannou, M. Kolosova, S. Konstantinou, G. Mavromanolakis, J. Mousa, C. Nicolaou, F. Ptochos, P.A. Razis, H. Rykaczewski, D. Tsiakkouri

University of Cyprus, Nicosia, Cyprus

M. Finger⁹, M. Finger Jr.⁹

Charles University, Prague, Czech Republic

E. Ayala

Escuela Politecnica Nacional, Quito, Ecuador

E. Carrera Jarrin

Universidad San Francisco de Quito, Quito, Ecuador

H. Abdalla¹⁰, A.A. Abdelalim^{11,12}

Academy of Scientific Research and Technology of the Arab Republic of Egypt, Egyptian Network of High Energy Physics, Cairo, Egypt

S. Bhowmik, A. Carvalho Antunes De Oliveira, R.K. Dewanjee, K. Ehataht, M. Kadastik, M. Raidal, C. Veelken

National Institute of Chemical Physics and Biophysics, Tallinn, Estonia

P. Eerola, H. Kirschenmann, K. Osterberg, J. Pekkanen, M. Voutilainen

Department of Physics, University of Helsinki, Helsinki, Finland

F. Garcia, J. Havukainen, J.K. Heikkilä, T. Järvinen, V. Karimäki, R. Kinnunen, T. Lampén, K. Lassila-Perini, S. Laurila, S. Lehti, T. Lindén, P. Luukka, T. Mäenpää, H. Siikonen, E. Tuominen, J. Tuominiemi

Helsinki Institute of Physics, Helsinki, Finland

T. Tuuva

Lappeenranta University of Technology, Lappeenranta, Finland

M. Besancon, F. Couderc, M. Dejardin, D. Denegri, B. Fabbro, J.L. Faure, F. Ferri, S. Ganjour, A. Givernaud, P. Gras, G. Hamel de Monchenault, P. Jarry, C. Leloup, E. Locci, J. Malcles, J. Rander, A. Rosowsky, M.Ö. Sahin, A. Savoy-Navarro¹³, M. Titov

IRFU, CEA, Université Paris-Saclay, Gif-sur-Yvette, France

C. Amendola, F. Beaudette, P. Busson, C. Charlot, B. Diab, R. Granier de Cassagnac, I. Kucher, A. Lobanov, C. Martin Perez, M. Nguyen, C. Ochando, P. Paganini, J. Rembser, R. Salerno, J.B. Sauvan, Y. Sirois, A. Zabi, A. Zghiche

Laboratoire Leprince-Ringuet, Ecole polytechnique, CNRS/IN2P3, Université Paris-Saclay, Palaiseau, France

J.-L. Agram¹⁴, J. Andrea, D. Bloch, G. Bourgatte, J.-M. Brom, E.C. Chabert, C. Collard, E. Conte¹⁴, J.-C. Fontaine¹⁴, D. Gelé, U. Goerlach, M. Jansová, A.-C. Le Bihan, N. Tonon, P. Van Hove

Université de Strasbourg, CNRS, IPHC UMR 7178, Strasbourg, France

S. Gadrat

Centre de Calcul de l'Institut National de Physique Nucleaire et de Physique des Particules, CNRS/IN2P3, Villeurbanne, France

S. Beauceron, C. Bernet, G. Boudoul, C. Camen, N. Chanon, R. Chierici, D. Contardo, P. Depasse, H. El Mamouni, J. Fay, S. Gascon, M. Gouzevitch, B. Ille, Sa. Jain, F. Lagarde, I.B. Laktineh, H. Lattaud, M. Lethuillier, L. Mirabito, S. Perries, V. Sordini, G. Touquet, M. Vander Donckt, S. Viret

Université de Lyon, Université Claude Bernard Lyon 1, CNRS-IN2P3, Institut de Physique Nucléaire de Lyon, Villeurbanne, France

A. Khvedelidze⁹

Georgian Technical University, Tbilisi, Georgia

Z. Tsamalaidze⁹

Tbilisi State University, Tbilisi, Georgia

C. Autermann, L. Feld, M.K. Kiesel, K. Klein, M. Lipinski, D. Meuser, A. Pauls, M. Preuten, M.P. Rauch, C. Schomakers, J. Schulz, M. Teroerde, B. Wittmer

RWTH Aachen University, I. Physikalisches Institut, Aachen, Germany

A. Albert, M. Erdmann, S. Erdweg, T. Esch, B. Fischer, R. Fischer, S. Ghosh, T. Hebbeker, K. Hoepfner, H. Keller, L. Mastrolorenzo, M. Merschmeyer, A. Meyer, P. Millet, G. Mocellin, S. Mondal, S. Mukherjee, D. Noll, A. Novak, T. Pook, A. Pozdnyakov, T. Quast, M. Radziej, Y. Rath, H. Reithler, M. Rieger, A. Schmidt, S.C. Schuler, A. Sharma, S. Thüer, S. Wiedenbeck

RWTH Aachen University, III. Physikalisches Institut A, Aachen, Germany

G. Flügge, O. Hlushchenko, T. Kress, T. Müller, A. Nehrkorn, A. Nowack, C. Pistone, O. Pooth, D. Roy, H. Sert, A. Stahl¹⁵

RWTH Aachen University, III. Physikalisches Institut B, Aachen, Germany

M. Aldaya Martin, C. Asawatangtrakuldee, P. Asmuss, I. Babounikau, H. Bakhshiansohi, K. Beernaert, O. Behnke, U. Behrens, A. Bermúdez Martínez, D. Bertsche, A.A. Bin Anuar, K. Borras¹⁶, V. Botta, A. Campbell, A. Cardini, P. Connor, S. Consuegra Rodríguez, C. Contreras-Campana, V. Danilov, A. De Wit, M.M. Defranchis, C. Diez Pardos, D. Domínguez Damiani, G. Eckerlin, D. Eckstein, T. Eichhorn, A. Elwood, E. Eren, E. Gallo¹⁷, A. Geiser, J.M. Grados Luyando, A. Grohsjean, M. Guthoff, M. Haranko, A. Harb, N.Z. Jomhari, H. Jung, A. Kasem¹⁶, M. Kasemann, J. Keaveney, C. Kleinwort, J. Knolle, D. Krücker, W. Lange, T. Lenz, J. Leonard, J. Lidrych, K. Lipka, W. Lohmann¹⁸, R. Mankel, I.-A. Melzer-Pellmann, A.B. Meyer, M. Meyer, M. Missiroli, G. Mittag, J. Mnich, A. Mussgiller, V. Myronenko, D. Pérez Adán, S.K. Pflitsch, D. Pitzl, A. Raspereza, A. Saibel, M. Savitskyi, V. Scheurer, P. Schütze, C. Schwanenberger,

R. Shevchenko, A. Singh, H. Tholen, O. Turkot, A. Vagnerini, M. Van De Klundert, G.P. Van Onsem, R. Walsh, Y. Wen, K. Wichmann, C. Wissing, O. Zenaiev, R. Zlebcik

Deutsches Elektronen-Synchrotron, Hamburg, Germany

R. Aggleton, S. Bein, L. Benato, A. Benecke, V. Blobel, T. Dreyer, A. Ebrahimi, A. Fröhlich, C. Garbers, E. Garutti, D. Gonzalez, P. Gunnellini, J. Haller, A. Hinzmann, A. Karavdina, G. Kasieczka, R. Klanner, R. Kogler, N. Kovalchuk, S. Kurz, V. Kutzner, J. Lange, T. Lange, A. Malara, D. Marconi, J. Multhaup, M. Niedziela, C.E.N. Niemeyer, D. Nowatschin, A. Perieanu, A. Reimers, O. Rieger, C. Scharf, P. Schleper, S. Schumann, J. Schwandt, J. Sonneveld, H. Stadie, G. Steinbrück, F.M. Stober, M. Stöver, B. Vormwald, I. Zoi

University of Hamburg, Hamburg, Germany

M. Akbiyik, C. Barth, M. Baselga, S. Baur, T. Berger, E. Butz, R. Caspart, T. Chwalek, W. De Boer, A. Dierlamm, K. El Morabit, N. Faltermann, M. Giffels, P. Goldenzweig, M.A. Harrendorf, F. Hartmann¹⁵, U. Husemann, S. Kudella, S. Mitra, M.U. Mozer, Th. Müller, M. Musich, A. Nürnberg, G. Quast, K. Rabbertz, M. Schröder, I. Shvetsov, H.J. Simonis, R. Ulrich, M. Weber, C. Wöhrmann, R. Wolf

Karlsruher Institut fuer Technologie, Karlsruhe, Germany

G. Anagnostou, P. Asenov, G. Daskalakis, T. Gerasis, A. Kyriakis, D. Loukas, G. Paspalaki

Institute of Nuclear and Particle Physics (INPP), NCSR Demokritos, Aghia Paraskevi, Greece

M. Diamantopoulou, G. Karathanasis, P. Kontaxakis, A. Panagiotou, I. Papavergou, N. Saoulidou, K. Theofilatos, K. Vellidis

National and Kapodistrian University of Athens, Athens, Greece

G. Bakas, K. Kousouris, I. Papakrivopoulos, G. Tsipolitis

National Technical University of Athens, Athens, Greece

I. Evangelou, C. Foudas, P. Gianneios, P. Katsoulis, P. Kokkas, S. Mallios, K. Manitaras, N. Manthos, I. Papadopoulos, E. Paradas, J. Strologas, F.A. Triantis, D. Tsitsonis

University of Ioánnina, Ioánnina, Greece

M. Bartók¹⁹, M. Csanad, P. Major, K. Mandal, A. Mehta, M.I. Nagy, G. Pasztor, O. Surányi, G.I. Veres

MTA-ELTE Lendület CMS Particle and Nuclear Physics Group, Eötvös Loránd University, Budapest, Hungary

G. Bencze, C. Hajdu, D. Horvath²⁰, Á. Hunyadi, F. Sikler, T.Á. Vámi, V. Veszpremi, G. Vesztergombi[†]

Wigner Research Centre for Physics, Budapest, Hungary

N. Beni, S. Czellar, J. Karancsi¹⁹, A. Makovec, J. Molnar, Z. Szillasi

Institute of Nuclear Research ATOMKI, Debrecen, Hungary

P. Raics, D. Teyssier, Z.L. Trocsanyi, B. Ujvari

Institute of Physics, University of Debrecen, Debrecen, Hungary

T.F. Csorgo, F. Nemes, T. Novak

Eszterhazy Karoly University, Karoly Robert Campus, Gyongyos, Hungary

S. Choudhury, J.R. Komaragiri, P.C. Tiwari

Indian Institute of Science (IISc), Bangalore, India

S. Bahinipati²², C. Kar, G. Kole, P. Mal, V.K. Muraleedharan Nair Bindhu, A. Nayak²³, S. Roy Chowdhury, D.K. Sahoo²², S.K. Swain

National Institute of Science Education and Research, HBNI, Bhubaneswar, India

S. Bansal, S.B. Beri, V. Bhatnagar, S. Chauhan, R. Chawla, N. Dhingra, R. Gupta, A. Kaur, M. Kaur, S. Kaur, P. Kumari, M. Lohan, M. Meena, K. Sandeep, S. Sharma, J.B. Singh, A.K. Virdi, G. Walia

Panjab University, Chandigarh, India

A. Bhardwaj, B.C. Choudhary, R.B. Garg, M. Gola, S. Keshri, Ashok Kumar, S. Malhotra, M. Naimuddin, P. Priyanka, K. Ranjan, Aashaq Shah, R. Sharma

University of Delhi, Delhi, India

R. Bhardwaj²⁴, M. Bharti²⁴, R. Bhattacharya, S. Bhattacharya, U. Bhawandeep²⁴, D. Bhowmik, S. Dey, S. Dutta, S. Ghosh, M. Maity²⁵, K. Mondal, S. Nandan, A. Purohit, P.K. Rout, A. Roy, G. Saha, S. Sarkar, T. Sarkar²⁵, M. Sharan, B. Singh²⁴, S. Thakur²⁴

Saha Institute of Nuclear Physics, HBNI, Kolkata, India

P.K. Behera, A. Muhammad

Indian Institute of Technology Madras, Madras, India

R. Chudasama, D. Dutta, V. Jha, V. Kumar, D.K. Mishra, P.K. Netrakanti, L.M. Pant, P. Shukla

Bhabha Atomic Research Centre, Mumbai, India

T. Aziz, M.A. Bhat, S. Dugad, G.B. Mohanty, N. Sur, RavindraKumar Verma

Tata Institute of Fundamental Research - A, Mumbai, India

S. Banerjee, S. Bhattacharya, S. Chatterjee, P. Das, M. Guchait, S. Karmakar, S. Kumar, G. Majumder, K. Mazumdar, N. Sahoo, S. Sawant

Tata Institute of Fundamental Research - B, Mumbai, India

S. Chauhan, S. Dube, V. Hegde, A. Kapoor, K. Kothekar, S. Pandey, A. Rane, A. Rastogi, S. Sharma

Indian Institute of Science Education and Research (IISER), Pune, India

S. Chenarani²⁶, E. Eskandari Tadavani, S.M. Etesami²⁶, M. Khakzad, M. Mohammadi Najafabadi, M. Naseri, F. Rezaei Hosseinabadi, B. Safarzadeh²⁷

Institute for Research in Fundamental Sciences (IPM), Tehran, Iran

M. Felcini, M. Grunewald

University College Dublin, Dublin, Ireland

M. Abbrescia^{a,b}, C. Calabria^{a,b}, A. Colaleo^a, D. Creanza^{a,c}, L. Cristella^{a,b}, N. De Filippis^{a,c}, M. De Palma^{a,b}, A. Di Florio^{a,b}, F. Errico^{a,b}, L. Fiore^a, A. Gelmi^{a,b}, G. Iaselli^{a,c}, M. Ince^{a,b}, S. Lezki^{a,b}, G. Maggi^{a,c}, M. Maggi^a, S. My^{a,b}, S. Nuzzo^{a,b}, A. Pompili^{a,b}, G. Pugliese^{a,c}, R. Radogna^a, A. Ranieri^a, G. Selvaggi^{a,b}, L. Silvestris^a, R. Venditti^a, P. Verwilligen^a

^a INFN Sezione di Bari, Bari, Italy

^b Università di Bari, Bari, Italy

^c Politecnico di Bari, Bari, Italy

G. Abbiendi^a, C. Battilana^{a,b}, D. Bonacorsi^{a,b}, L. Borghonovi^{a,b}, S. Braibant-Giacomelli^{a,b}, R. Campanini^{a,b}, P. Capiluppi^{a,b}, A. Castro^{a,b}, F.R. Cavallo^a, S.S. Chhibra^{a,b}, C. Ciocca^a, G. Codispoti^{a,b}, M. Cuffiani^{a,b}, G.M. Dallavalle^a, F. Fabbri^a, A. Fanfani^{a,b}, E. Fontanesi, P. Giacomelli^a, C. Grandi^a,

L. Guiducci^{a,b}, F. Iemmi^{a,b}, S. Lo Meo^{a,28}, S. Marcellini^a, G. Masetti^a, F.L. Navarria^{a,b}, A. Perrotta^a, F. Primavera^{a,b}, A.M. Rossi^{a,b}, T. Rovelli^{a,b}, G.P. Siroli^{a,b}, N. Tosi^a

^a INFN Sezione di Bologna, Bologna, Italy

^b Università di Bologna, Bologna, Italy

S. Albergo^{a,b,29}, S. Costa^{a,b}, A. Di Mattia^a, R. Potenza^{a,b}, A. Tricomi^{a,b,29}, C. Tuve^{a,b}

^a INFN Sezione di Catania, Catania, Italy

^b Università di Catania, Catania, Italy

G. Barbagli^a, R. Ceccarelli, K. Chatterjee^{a,b}, V. Ciulli^{a,b}, C. Civinini^a, R. D'Alessandro^{a,b}, E. Focardi^{a,b}, G. Latino, P. Lenzi^{a,b}, M. Meschini^a, S. Paoletti^a, L. Russo^{a,30}, G. Sguazzoni^a, D. Strom^a, L. Viliani^a

^a INFN Sezione di Firenze, Firenze, Italy

^b Università di Firenze, Firenze, Italy

L. Benussi, S. Bianco, F. Fabbri, D. Piccolo

INFN Laboratori Nazionali di Frascati, Frascati, Italy

M. Bozzo^{a,b}, F. Ferro^a, R. Mulargia^{a,b}, E. Robutti^a, S. Tosi^{a,b}

^a INFN Sezione di Genova, Genova, Italy

^b Università di Genova, Genova, Italy

A. Benaglia^a, A. Beschi^b, F. Brivio^{a,b}, V. Ciriolo^{a,b,15}, S. Di Guida^{a,b,15}, M.E. Dinardo^{a,b}, P. Dini^a, S. Fiorendi^{a,b}, S. Gennai^a, A. Ghezzi^{a,b}, P. Govoni^{a,b}, M. Malberti^{a,b}, S. Malvezzi^a, D. Menasce^a, F. Monti, L. Moroni^a, G. Ortona^{a,b}, M. Paganoni^{a,b}, D. Pedrini^a, S. Ragazzi^{a,b}, T. Tabarelli de Fatis^{a,b}, D. Zuolo^{a,b}

^a INFN Sezione di Milano–Bicocca, Milano, Italy

^b Università di Milano–Bicocca, Milano, Italy

S. Buontempo^a, N. Cavallo^{a,c}, A. De Iorio^{a,b}, A. Di Crescenzo^{a,b}, F. Fabozzi^{a,c}, F. Fienga^a, G. Galati^a, A.O.M. Iorio^{a,b}, L. Lista^{a,b}, S. Meola^{a,d,15}, P. Paolucci^{a,15}, C. Sciacca^{a,b}, E. Voevodina^{a,b}

^a INFN Sezione di Napoli, Napoli, Italy

^b Università di Napoli ‘Federico II’, Napoli, Italy

^c Università della Basilicata, Potenza, Italy

^d Università G. Marconi, Roma, Italy

P. Azzi^a, N. Bacchetta^a, D. Bisello^{a,b}, A. Boletti^{a,b}, A. Bragagnolo, R. Carlin^{a,b}, P. Checchia^a, M. Dall’Osso^{a,b}, P. De Castro Manzano^a, T. Dorigo^a, U. Dosselli^a, F. Gasparini^{a,b}, U. Gasparini^{a,b}, A. Gozzelino^a, S.Y. Hoh, P. Lujan, M. Margoni^{a,b}, A.T. Meneguzzo^{a,b}, J. Pazzini^{a,b}, M. Presilla^b, P. Ronchese^{a,b}, R. Rossin^{a,b}, F. Simonetto^{a,b}, A. Tiko, M. Tosi^{a,b}, M. Zanetti^{a,b}, P. Zotto^{a,b}, G. Zumerle^{a,b}

^a INFN Sezione di Padova, Padova, Italy

^b Università di Padova, Padova, Italy

^c Università di Trento, Trento, Italy

A. Braghieri^a, P. Montagna^{a,b}, S.P. Ratti^{a,b}, V. Re^a, M. Ressegotti^{a,b}, C. Riccardi^{a,b}, P. Salvini^a, I. Vai^{a,b}, P. Vitulo^{a,b}

^a INFN Sezione di Pavia, Pavia, Italy

^b Università di Pavia, Pavia, Italy

M. Biasini^{a,b}, G.M. Bilei^a, C. Cecchi^{a,b}, D. Ciangottini^{a,b}, L. Fanò^{a,b}, P. Lariccia^{a,b}, R. Leonardi^{a,b}, E. Manoni^a, G. Mantovani^{a,b}, V. Mariani^{a,b}, M. Menichelli^a, A. Rossi^{a,b}, A. Santocchia^{a,b}, D. Spiga^a

^a INFN Sezione di Perugia, Perugia, Italy

^b Università di Perugia, Perugia, Italy

K. Androsov^a, P. Azzurri^a, G. Bagliesi^a, V. Bertacchi^{a,c}, L. Bianchini^a, T. Boccali^a, R. Castaldi^a, M.A. Ciocci^{a,b}, R. Dell’Orso^a, G. Fedi^a, F. Fiori^{a,c}, L. Giannini^{a,c}, A. Giassi^a, M.T. Grippo^a, F. Ligabue^{a,c}

E. Manca ^{a,c}, G. Mandorli ^{a,c}, A. Messineo ^{a,b}, F. Palla ^a, A. Rizzi ^{a,b}, G. Rolandi ³¹, A. Scribano ^a, P. Spagnolo ^a, R. Tenchini ^a, G. Tonelli ^{a,b}, N. Turini, A. Venturi ^a, P.G. Verдини ^a

^a INFN Sezione di Pisa, Pisa, Italy

^b Università di Pisa, Pisa, Italy

^c Scuola Normale Superiore di Pisa, Pisa, Italy

F. Cavallari ^a, M. Cipriani ^{a,b}, D. Del Re ^{a,b}, E. Di Marco ^{a,b}, M. Diemoz ^a, S. Gelli ^{a,b}, E. Longo ^{a,b}, B. Marzocchi ^{a,b}, P. Meridiani ^a, G. Organtini ^{a,b}, F. Pandolfi ^a, R. Paramatti ^{a,b}, F. Preiato ^{a,b}, C. Quaranta ^{a,b}, S. Rahatlou ^{a,b}, C. Rovelli ^a, F. Santanastasio ^{a,b}, L. Soffi ^{a,b}

^a INFN Sezione di Roma, Rome, Italy

^b Sapienza Università di Roma, Rome, Italy

N. Amapane ^{a,b}, R. Arcidiacono ^{a,c}, S. Argiro ^{a,b}, M. Arneodo ^{a,c}, N. Bartosik ^a, R. Bellan ^{a,b}, C. Biino ^a, A. Cappati ^{a,b}, N. Cartiglia ^a, F. Cenna ^{a,b}, S. Cometti ^a, M. Costa ^{a,b}, R. Covarelli ^{a,b}, N. Demaria ^a, B. Kiani ^{a,b}, C. Mariotti ^a, S. Maselli ^a, E. Migliore ^{a,b}, V. Monaco ^{a,b}, E. Monteil ^{a,b}, M. Monteno ^a, M.M. Obertino ^{a,b}, L. Pacher ^{a,b}, N. Pastrone ^a, M. Pelliccioni ^a, G.L. Pinna Angioni ^{a,b}, A. Romero ^{a,b}, M. Ruspa ^{a,c}, R. Sacchi ^{a,b}, R. Salvatico ^{a,b}, K. Shchelina ^{a,b}, V. Sola ^a, A. Solano ^{a,b}, D. Soldi ^{a,b}, A. Staiano ^a

^a INFN Sezione di Torino, Torino, Italy

^b Università di Torino, Torino, Italy

^c Università del Piemonte Orientale, Novara, Italy

S. Belforte ^a, V. Candelise ^{a,b}, M. Casarsa ^a, F. Cossutti ^a, A. Da Rold ^{a,b}, G. Della Ricca ^{a,b}, F. Vazzoler ^{a,b}, A. Zanetti ^a

^a INFN Sezione di Trieste, Trieste, Italy

^b Università di Trieste, Trieste, Italy

B. Kim, D.H. Kim, G.N. Kim, M.S. Kim, J. Lee, S.W. Lee, C.S. Moon, Y.D. Oh, S.I. Pak, S. Sekmen, D.C. Son, Y.C. Yang

Kyungpook National University, Daegu, Republic of Korea

H. Kim, D.H. Moon, G. Oh

Chonnam National University, Institute for Universe and Elementary Particles, Kwangju, Republic of Korea

B. Francois, T.J. Kim, J. Park

Hanyang University, Seoul, Republic of Korea

S. Cho, S. Choi, Y. Go, D. Gyun, S. Ha, B. Hong, Y. Jo, K. Lee, K.S. Lee, S. Lee, J. Lim, J. Park, S.K. Park, Y. Roh

Korea University, Seoul, Republic of Korea

J. Goh

Kyung Hee University, Department of Physics, South Korea

H.S. Kim

Sejong University, Seoul, Republic of Korea

J. Almond, J.H. Bhyun, J. Choi, S. Jeon, J. Kim, J.S. Kim, H. Lee, K. Lee, S. Lee, K. Nam, S.B. Oh, B.C. Radburn-Smith, S.h. Seo, U.K. Yang, H.D. Yoo, I. Yoon, G.B. Yu

Seoul National University, Seoul, Republic of Korea

D. Jeon, H. Kim, J.H. Kim, J.S.H. Lee, I.C. Park

University of Seoul, Seoul, Republic of Korea

Y. Choi, C. Hwang, Y. Jeong, J. Lee, Y. Lee, I. Yu

Sungkyunkwan University, Suwon, Republic of Korea

V. Veckalns³²

Riga Technical University, Riga, Latvia

V. Dudenas, A. Juodagalvis, J. Vaitkus

Vilnius University, Vilnius, Lithuania

Z.A. Ibrahim, F. Mohamad Idris³³, W.A.T. Wan Abdullah, M.N. Yusli, Z. Zolkapli

National Centre for Particle Physics, Universiti Malaya, Kuala Lumpur, Malaysia

J.F. Benitez, A. Castaneda Hernandez, J.A. Murillo Quijada, L. Valencia Palomo

Universidad de Sonora (UNISON), Hermosillo, Mexico

H. Castilla-Valdez, E. De La Cruz-Burelo, M.C. Duran-Osuna, I. Heredia-De La Cruz³⁴, R. Lopez-Fernandez, R.I. Rabadan-Trejo, G. Ramirez-Sanchez, R. Reyes-Almanza, A. Sanchez-Hernandez

Centro de Investigacion y de Estudios Avanzados del IPN, Mexico City, Mexico

S. Carrillo Moreno, C. Oropeza Barrera, M. Ramirez-Garcia, F. Vazquez Valencia

Universidad Iberoamericana, Mexico City, Mexico

J. Eysermans, I. Pedraza, H.A. Salazar Ibarguen, C. Uribe Estrada

Benemerita Universidad Autonoma de Puebla, Puebla, Mexico

A. Morelos Pineda

Universidad Autónoma de San Luis Potosí, San Luis Potosí, Mexico

N. Raicevic

University of Montenegro, Podgorica, Montenegro

D. Krofcheck

University of Auckland, Auckland, New Zealand

S. Bheesette, P.H. Butler

University of Canterbury, Christchurch, New Zealand

A. Ahmad, M. Ahmad, Q. Hassan, H.R. Hoorani, W.A. Khan, M.A. Shah, M. Shoaib, M. Waqas

National Centre for Physics, Quaid-I-Azam University, Islamabad, Pakistan

V. Avati, L. Grzanka, M. Malawski

AGH University of Science and Technology Faculty of Computer Science, Electronics and Telecommunications, Krakow, Poland

H. Bialkowska, M. Bluj, B. Boimska, M. Górski, M. Kazana, M. Szleper, P. Zalewski

National Centre for Nuclear Research, Swierk, Poland

K. Bunkowski, A. Byszuk³⁵, K. Doroba, A. Kalinowski, M. Konecki, J. Krolikowski, M. Misiura, M. Olszewski, A. Pyskir, M. Walczak

Institute of Experimental Physics, Faculty of Physics, University of Warsaw, Warsaw, Poland

M. Araujo, P. Bargassa, D. Bastos, A. Di Francesco, P. Faccioli, B. Galinhas, M. Gallinaro, J. Hollar, N. Leonardo, J. Seixas, G. Strong, O. Toldaiev, J. Varela

Laboratório de Instrumentação e Física Experimental de Partículas, Lisboa, Portugal

P. Bunin, M. Gavrilenko, A. Golunov, A. Golunov, I. Golutvin, I. Gorbunov, V. Karjavine, V. Korenkov, A. Lanev, A. Malakhov, V. Matveev^{36,37}, P. Moisenz, V. Palichik, V. Pereygin, M. Savina, S. Shmatov, S. Shulha, O. Teryaev, N. Voytishin, A. Zarubin

Joint Institute for Nuclear Research, Dubna, Russia

L. Chtchipounov, V. Golovtsov, Y. Ivanov, V. Kim³⁸, E. Kuznetsova³⁹, P. Levchenko, V. Murzin, V. Oreshkin, I. Smirnov, D. Sosnov, V. Sulimov, L. Uvarov, A. Vorobyev

Petersburg Nuclear Physics Institute, Gatchina (St. Petersburg), Russia

Yu. Andreev, A. Dermenev, S. Gninenko, N. Golubev, A. Karneyeu, M. Kirsanov, N. Krasnikov, A. Pashenkov, D. Tisov, A. Toropin

Institute for Nuclear Research, Moscow, Russia

V. Epshteyn, V. Gavrilov, N. Lychkovskaya, A. Nikitenko⁸, V. Popov, I. Pozdnyakov, G. Safronov, A. Spiridonov, A. Stepenov, M. Toms, E. Vlasov, A. Zhokin

Institute for Theoretical and Experimental Physics named by A.I. Alikhanov of NRC 'Kurchatov Institute', Moscow, Russia

T. Aushev

Moscow Institute of Physics and Technology, Moscow, Russia

R. Chistov⁴⁰, M. Danilov⁴⁰, D. Philippov, E. Tarkovskii

National Research Nuclear University 'Moscow Engineering Physics Institute' (MEPhI), Moscow, Russia

V. Andreev, M. Azarkin, I. Dremin³⁷, M. Kirakosyan, A. Terkulov

P.N. Lebedev Physical Institute, Moscow, Russia

A. Belyaev, E. Boos, V. Bunichev, M. Dubinin⁴¹, L. Dudko, A. Gribushin, V. Klyukhin, O. Kodolova, I. Lokhtin, S. Obraztsov, M. Perfilov, S. Petrushanko, V. Savrin

Skobeltsyn Institute of Nuclear Physics, Lomonosov Moscow State University, Moscow, Russia

A. Barnyakov⁴², V. Blinov⁴², T. Dimova⁴², L. Kardapoltsev⁴², Y. Skovpen⁴²

Novosibirsk State University (NSU), Novosibirsk, Russia

I. Azhgirey, I. Bayshev, S. Bitioukov, V. Kachanov, D. Konstantinov, P. Mandrik, V. Petrov, R. Ryutin, S. Slabospitskii, A. Sobol, S. Troshin, N. Tyurin, A. Uzunian, A. Volkov

Institute for High Energy Physics of National Research Centre 'Kurchatov Institute', Protvino, Russia

A. Babaev, A. Iuzhakov, V. Okhotnikov

National Research Tomsk Polytechnic University, Tomsk, Russia

V. Borchsh, V. Ivantchenko, E. Tcherniaev

Tomsk State University, Tomsk, Russia

P. Adzic⁴³, P. Cirkovic, D. Devetak, M. Dordevic, P. Milenovic⁴⁴, J. Milosevic, M. Stojanovic

University of Belgrade: Faculty of Physics and VINCA Institute of Nuclear Sciences, Serbia

M. Aguilar-Benitez, J. Alcaraz Maestre, A. Álvarez Fernández, I. Bachiller, M. Barrio Luna, J.A. Brochero Cifuentes, C.A. Carrillo Montoya, M. Cepeda, M. Cerrada, N. Colino, B. De La Cruz, A. Delgado Peris, C. Fernandez Bedoya, J.P. Fernández Ramos, J. Flix, M.C. Fouz, O. Gonzalez Lopez,

S. Goy Lopez, J.M. Hernandez, M.I. Josa, D. Moran, Á. Navarro Tobar, A. Pérez-Calero Yzquierdo, J. Puerta Pelayo, I. Redondo, L. Romero, S. Sánchez Navas, M.S. Soares, A. Triossi, C. Willmott

Centro de Investigaciones Energéticas Medioambientales y Tecnológicas (CIEMAT), Madrid, Spain

C. Albajar, J.F. de Trocóniz

Universidad Autónoma de Madrid, Madrid, Spain

J. Cuevas, C. Erice, J. Fernandez Menendez, S. Folgueras, I. Gonzalez Caballero, J.R. González Fernández, E. Palencia Cortezon, V. Rodríguez Bouza, S. Sanchez Cruz, J.M. Vizan Garcia

Universidad de Oviedo, Instituto Universitario de Ciencias y Tecnologías Espaciales de Asturias (ICTEA), Spain

I.J. Cabrillo, A. Calderon, B. Chazin Quero, J. Duarte Campderros, M. Fernandez, P.J. Fernández Manteca, A. García Alonso, G. Gomez, A. Lopez Virto, C. Martinez Rivero, P. Martinez Ruiz del Arbol, F. Matorras, J. Piedra Gomez, C. Prieels, T. Rodrigo, A. Ruiz-Jimeno, L. Scodellaro, N. Trevisani, I. Vila

Instituto de Física de Cantabria (IFCA), CSIC-Universidad de Cantabria, Santander, Spain

K. Malagalage

University of Colombo, Colombo, Sri Lanka

W.G.D. Dharmaratna, N. Wickramage

University of Ruhuna, Department of Physics, Matara, Sri Lanka

D. Abbaneo, B. Akgun, E. Auffray, G. Auzinger, J. Baechler, P. Baillon[†], A.H. Ball, D. Barney, J. Bendavid, M. Bianco, A. Bocci, E. Bossini, C. Botta, E. Brondolin, T. Camporesi, A. Caratelli, G. Cerminara, E. Chapon, G. Cucciati, D. d'Enterria, A. Dabrowski, N. Daci, V. Daponte, A. David, A. De Roeck, N. Deelen, M. Deile, M. Dobson, M. Dünser, N. Dupont, A. Elliott-Peisert, F. Fallavollita⁴⁵, D. Fasanella, G. Franzoni, J. Fulcher, W. Funk, S. Giani, D. Gigi, A. Gilbert, K. Gill, F. Glege, M. Gruchala, M. Guilbaud, D. Gulhan, J. Hegeman, C. Heidegger, Y. Iiyama, V. Innocente, A. Jafari, P. Janot, O. Karacheban¹⁸, J. Kaspar, J. Kieseler, M. Krammer¹, C. Lange, P. Lecoq, C. Lourenço, L. Malgeri, M. Mannelli, A. Massironi, F. Meijers, J.A. Merlin, S. Mersi, E. Meschi, F. Moortgat, M. Mulders, J. Ngadiuba, S. Nourbakhsh, S. Orfanelli, L. Orsini, F. Pantaleo¹⁵, L. Pape, E. Perez, M. Peruzzi, A. Petrilli, G. Petrucciani, A. Pfeiffer, M. Pierini, F.M. Pitters, M. Quinto, D. Rabady, A. Racz, M. Rovere, H. Sakulin, C. Schäfer, C. Schwick, M. Selvaggi, A. Sharma, P. Silva, W. Snoeys, P. Sphicas⁴⁶, A. Stakia, J. Steggemann, V.R. Tavolaro, D. Treille, A. Tsiros, A. Vartak, M. Verzetti, W.D. Zeuner

CERN, European Organization for Nuclear Research, Geneva, Switzerland

L. Caminada⁴⁷, K. Deiters, W. Erdmann, R. Horisberger, Q. Ingram, H.C. Kaestli, D. Kotlinski, U. Langenegger, T. Rohe, S.A. Wiederkehr

Paul Scherrer Institut, Villigen, Switzerland

M. Backhaus, P. Berger, N. Chernyavskaya, G. Dissertori, M. Dittmar, M. Donegà, C. Dorfer, T.A. Gómez Espinosa, C. Grab, D. Hits, T. Klijnsma, W. Lustermann, R.A. Manzoni, M. Marionneau, M.T. Meinhard, F. Micheli, P. Musella, F. Nessi-Tedaldi, F. Pauss, G. Perrin, L. Perrozzi, S. Pigazzini, M. Reichmann, C. Reissel, T. Reitenspiess, D. Ruini, D.A. Sanz Becerra, M. Schönenberger, L. Shchutska, M.L. Vesterbacka Olsson, R. Wallny, D.H. Zhu

ETH Zurich – Institute for Particle Physics and Astrophysics (IPA), Zurich, Switzerland

T.K. Aarrestad, C. AMSler⁴⁸, D. Brzhechko, M.F. Canelli, A. De Cosa, R. Del Burgo, S. Donato, C. Galloni, B. Kilminster, S. Leontsinis, V.M. Mikuni, I. Neutelings, G. Rauco, P. Robmann, D. Salerno, K. Schweiger, C. Seitz, Y. Takahashi, S. Wertz, A. Zucchetta

Universität Zürich, Zurich, Switzerland

T.H. Doan, C.M. Kuo, W. Lin, S.S. Yu

National Central University, Chung-Li, Taiwan

P. Chang, Y. Chao, K.F. Chen, P.H. Chen, W.-S. Hou, R.-S. Lu, E. Paganis, A. Psallidas, A. Steen

National Taiwan University (NTU), Taipei, Taiwan

B. Asavapibhop, N. Srimanobhas, N. Suwonjandee

Chulalongkorn University, Faculty of Science, Department of Physics, Bangkok, Thailand

A. Bat, F. Boran, S. Cerci⁴⁹, S. Damarseckin⁵⁰, Z.S. Demiroglu, F. Dolek, C. Dozen, I. Dumanoglu, G. Gokbulut, EmineGurpinar Guler⁵¹, Y. Guler, I. Hos⁵², C. Isik, E.E. Kangal⁵³, O. Kara, A. Kayis Topaksu, U. Kiminsu, M. Oglakci, G. Onengut, K. Ozdemir⁵⁴, S. Ozturk⁵⁵, A.E. Simsek, D. Sunar Cerci⁴⁹, U.G. Tok, S. Turkcapar, I.S. Zorbakir, C. Zorbilmez

Çukurova University, Physics Department, Science and Art Faculty, Adana, Turkey

B. Isildak⁵⁶, G. Karapinar⁵⁷, M. Yalvac

Middle East Technical University, Physics Department, Ankara, Turkey

I.O. Atakisi, E. Gülmez, M. Kaya⁵⁸, O. Kaya⁵⁹, B. Kaynak, Ö. Özçelik, S. Ozkorucuklu⁶⁰, S. Tekten, E.A. Yetkin⁶¹

Bogazici University, Istanbul, Turkey

A. Cakir, Y. Komurcu, S. Sen⁶²

Istanbul Technical University, Istanbul, Turkey

B. Grynyov

Institute for Scintillation Materials of National Academy of Science of Ukraine, Kharkov, Ukraine

L. Levchuk

National Scientific Center, Kharkov Institute of Physics and Technology, Kharkov, Ukraine

F. Ball, E. Bhal, S. Bologna, J.J. Brooke, D. Burns, E. Clement, D. Cussans, O. Davignon, H. Flacher, J. Goldstein, G.P. Heath, H.F. Heath, L. Kreczko, S. Paramesvaran, B. Penning, T. Sakuma, S. Seif El Nasr-Storey, D. Smith, V.J. Smith, J. Taylor, A. Titterton

University of Bristol, Bristol, United Kingdom

K.W. Bell, A. Belyaev⁶³, C. Brew, R.M. Brown, D. Cieri, D.J.A. Cockerill, J.A. Coughlan, K. Harder, S. Harper, J. Linacre, K. Manolopoulos, D.M. Newbold⁶⁴, E. Olaiya, D. Petyt, T. Reis, T. Schuh, C.H. Shepherd-Themistocleous, A. Thea, I.R. Tomalin, T. Williams, W.J. Womersley

Rutherford Appleton Laboratory, Didcot, United Kingdom

R. Bainbridge, P. Bloch, J. Borg, S. Breeze, O. Buchmuller, A. Bundock, Gurpreet Singh Chahal⁶⁵, D. Colling, P. Dauncey, G. Davies, M. Della Negra, R. Di Maria, P. Everaerts, G. Hall, G. Iles, T. James, M. Komm, C. Laner, L. Lyons, A.-M. Magnan, S. Malik, A. Martelli, V. Milosevic, J. Nash⁶⁶, V. Palladino, M. Pesaresi, D.M. Raymond, A. Richards, A. Rose, E. Scott, C. Seez, A. Shtipliyski, M. Stoye, T. Strebler, S. Summers, A. Tapper, K. Uchida, T. Virdee¹⁵, N. Wardle, D. Winterbottom, J. Wright, A.G. Zecchinelli, S.C. Zenz

Imperial College, London, United Kingdom

J.E. Cole, P.R. Hobson, A. Khan, P. Kyberd, C.K. Mackay, A. Morton, I.D. Reid, L. Teodorescu, S. Zahid

Brunel University, Uxbridge, United Kingdom

K. Call, J. Dittmann, K. Hatakeyama, C. Madrid, B. McMaster, N. Pastika, C. Smith

Baylor University, Waco, USA

R. Bartek, A. Dominguez

Catholic University of America, Washington, DC, USA

A. Buccilli, S.I. Cooper, C. Henderson, P. Rumerio, C. West

The University of Alabama, Tuscaloosa, USA

D. Arcaro, T. Bose, Z. Demiragli, D. Gastler, S. Girgis, D. Pinna, C. Richardson, J. Rohlf, D. Sperka, I. Suarez, L. Sulak, D. Zou

Boston University, Boston, USA

G. Benelli, B. Burklee, X. Coubez, D. Cutts, M. Hadley, J. Hakala, U. Heintz, J.M. Hogan⁶⁷, K.H.M. Kwok, E. Laird, G. Landsberg, J. Lee, Z. Mao, M. Narain, S. Sagir⁶⁸, R. Syarif, E. Usai, D. Yu

Brown University, Providence, USA

R. Band, C. Brainerd, R. Breedon, M. Calderon De La Barca Sanchez, M. Chertok, J. Conway, R. Conway, P.T. Cox, R. Erbacher, C. Flores, G. Funk, F. Jensen, W. Ko, O. Kukral, R. Lander, M. Mulhearn, D. Pellett, J. Pilot, M. Shi, D. Stolp, D. Taylor, K. Tos, M. Tripathi, Z. Wang, F. Zhang

University of California, Davis, Davis, USA

M. Bachtis, C. Bravo, R. Cousins, A. Dasgupta, A. Florent, J. Hauser, M. Ignatenko, N. Mccoll, S. Regnard, D. Saltzberg, C. Schnaible, V. Valuev

University of California, Los Angeles, USA

K. Burt, R. Clare, J.W. Gary, S.M.A. Ghiasi Shirazi, G. Hanson, G. Karapostoli, E. Kennedy, O.R. Long, M. Olmedo Negrete, M.I. Paneva, W. Si, L. Wang, H. Wei, S. Wimpenny, B.R. Yates, Y. Zhang

University of California, Riverside, Riverside, USA

J.G. Branson, P. Chang, S. Cittolin, M. Derdzinski, R. Gerosa, D. Gilbert, B. Hashemi, D. Klein, V. Krutelyov, J. Letts, M. Masciovecchio, S. May, S. Padhi, M. Pieri, V. Sharma, M. Tadel, F. Würthwein, A. Yagil, G. Zevi Della Porta

University of California, San Diego, La Jolla, USA

N. Amin, R. Bhandari, C. Campagnari, M. Citron, V. Dutta, M. Franco Sevilla, L. Gouskos, J. Incandela, B. Marsh, H. Mei, A. Ovcharova, H. Qu, J. Richman, U. Sarica, D. Stuart, S. Wang, J. Yoo

University of California, Santa Barbara – Department of Physics, Santa Barbara, USA

D. Anderson, A. Bornheim, J.M. Lawhorn, N. Lu, H.B. Newman, T.Q. Nguyen, J. Pata, M. Spiropulu, J.R. Vlimant, S. Xie, Z. Zhang, R.Y. Zhu

California Institute of Technology, Pasadena, USA

M.B. Andrews, T. Ferguson, T. Mudholkar, M. Paulini, M. Sun, I. Vorobiev, M. Weinberg

Carnegie Mellon University, Pittsburgh, USA

J.P. Cumalat, W.T. Ford, A. Johnson, E. MacDonald, T. Mulholland, R. Patel, A. Perloff, K. Stenson, K.A. Ulmer, S.R. Wagner

University of Colorado Boulder, Boulder, USA

J. Alexander, J. Chaves, Y. Cheng, J. Chu, A. Datta, A. Frankenthal, K. Mcdermott, N. Mirman, J.R. Patterson, D. Quach, A. Rinkevicius, A. Ryd, S.M. Tan, Z. Tao, J. Thom, P. Wittich, M. Zientek

Cornell University, Ithaca, USA

S. Abdullin, M. Albrow, M. Alyari, G. Apollinari, A. Apresyan, A. Apyan, S. Banerjee, L.A.T. Bauerdick, A. Beretvas, J. Berryhill, P.C. Bhat, K. Burkett, J.N. Butler, A. Canepa, G.B. Cerati, H.W.K. Cheung, F. Chlebana, M. Cremonesi, J. Duarte, V.D. Elvira, J. Freeman, Z. Gecse, E. Gottschalk, L. Gray, D. Green, S. Grünendahl, O. Gutsche, Allison Reinsvold Hall, J. Hanlon, R.M. Harris, S. Hasegawa, R. Heller, J. Hirschauer, Z. Hu, B. Jayatilaka, S. Jindariani, M. Johnson, U. Joshi, B. Klima, M.J. Kortelainen, B. Kreis, S. Lammel, J. Lewis, D. Lincoln, R. Lipton, M. Liu, T. Liu, J. Lykken, K. Maeshima, J.M. Marraffino, D. Mason, P. McBride, P. Merkel, S. Mrenna, S. Nahn, V. O'Dell, V. Papadimitriou, K. Pedro, C. Pena, G. Rakness, F. Ravera, L. Ristori, B. Schneider, E. Sexton-Kennedy, N. Smith, A. Soha, W.J. Spalding, L. Spiegel, S. Stoynev, J. Strait, N. Strobbe, L. Taylor, S. Tkaczyk, N.V. Tran, L. Uplegger, E.W. Vaandering, C. Vernieri, M. Verzocchi, R. Vidal, M. Wang, H.A. Weber

Fermi National Accelerator Laboratory, Batavia, USA

D. Acosta, P. Avery, P. Bortignon, D. Bourilkov, A. Brinkerhoff, L. Cadamuro, A. Carnes, V. Cherepanov, D. Curry, R.D. Field, S.V. Gleyzer, B.M. Joshi, M. Kim, J. Konigsberg, A. Korytov, K.H. Lo, P. Ma, K. Matchev, N. Menendez, G. Mitselmakher, D. Rosenzweig, K. Shi, J. Wang, S. Wang, X. Zuo

University of Florida, Gainesville, USA

Y.R. Joshi, S. Linn

Florida International University, Miami, USA

T. Adams, A. Askew, S. Hagopian, V. Hagopian, K.F. Johnson, R. Khurana, T. Kolberg, G. Martinez, T. Perry, H. Prosper, C. Schiber, R. Yohay

Florida State University, Tallahassee, USA

M.M. Baarmand, V. Bhopatkar, M. Hohlmann, D. Noonan, M. Rahmani, T. Roy, M. Saunders, F. Yumiceva

Florida Institute of Technology, Melbourne, USA

M.R. Adams, L. Apanasevich, D. Berry, R. Cavanaugh, X. Chen, S. Dittmer, O. Evdokimov, C.E. Gerber, D.A. Hangal, D.J. Hofman, K. Jung, C. Mills, M.B. Tonjes, N. Varelas, H. Wang, X. Wang, Z. Wu, J. Zhang

University of Illinois at Chicago (UIC), Chicago, USA

M. Alhusseini, B. Bilki⁵¹, W. Clarida, K. Dilsiz⁶⁹, S. Durgut, R.P. Gandrajula, M. Haytmyradov, V. Khristenko, O.K. Köseyan, J.-P. Merlo, A. Mestvirishvili, A. Moeller, J. Nachtman, H. Ogul⁷⁰, Y. Onel, F. Ozok⁷¹, A. Penzo, C. Snyder, E. Tiras, J. Wetzel

The University of Iowa, Iowa City, USA

B. Blumenfeld, A. Cocoros, N. Eminizer, D. Fehling, L. Feng, A.V. Gritsan, W.T. Hung, P. Maksimovic, J. Roskes, M. Swartz, M. Xiao

Johns Hopkins University, Baltimore, USA

A. Al-bataineh, C. Baldenegro Barrera, P. Baringer, A. Bean, S. Boren, A. Bylinkin, J. Castle, T. Isidori, S. Khalil, J. King, A. Kropivnitskaya, D. Majumder, W. Mcbrayer, N. Minafra, M. Murray, C. Rogan, C. Royon, S. Sanders, E. Schmitz, J.D. Tapia Takaki, Q. Wang, J. Williams

The University of Kansas, Lawrence, USA

S. Duric, A. Ivanov, K. Kaadze, D. Kim, Y. Maravin, D.R. Mendis, T. Mitchell, A. Modak, A. Mohammadi

Kansas State University, Manhattan, USA

F. Rebassoo, D. Wright

Lawrence Livermore National Laboratory, Livermore, USA

A. Baden, O. Baron, A. Belloni, S.C. Eno, Y. Feng, C. Ferraioli, N.J. Hadley, S. Jabeen, G.Y. Jeng, R.G. Kellogg, J. Kunkle, A.C. Mignerey, S. Nabili, F. Ricci-Tam, M. Seidel, Y.H. Shin, A. Skuja, S.C. Tonwar, K. Wong

University of Maryland, College Park, USA

D. Abercrombie, B. Allen, A. Baty, R. Bi, S. Brandt, W. Busza, I.A. Cali, M. D'Alfonso, G. Gomez Ceballos, M. Goncharov, P. Harris, D. Hsu, M. Hu, M. Klute, D. Kovalskyi, Y.-J. Lee, P.D. Luckey, B. Maier, A.C. Marini, C. McGinn, C. Mironov, S. Narayanan, X. Niu, C. Paus, D. Rankin, C. Roland, G. Roland, Z. Shi, G.S.F. Stephens, K. Sumorok, K. Tatar, D. Velicanu, J. Wang, T.W. Wang, B. Wyslouch

Massachusetts Institute of Technology, Cambridge, USA

A.C. Benvenuti[†], R.M. Chatterjee, A. Evans, P. Hansen, J. Hiltbrand, S. Kalafut, Y. Kubota, Z. Lesko, J. Mans, R. Rusack, M.A. Wadud

University of Minnesota, Minneapolis, USA

J.G. Acosta, S. Oliveros

University of Mississippi, Oxford, USA

E. Avdeeva, K. Bloom, D.R. Claes, C. Fangmeier, L. Finco, F. Golf, R. Gonzalez Suarez, R. Kamalieddin, I. Kravchenko, J.E. Siado, G.R. Snow, B. Stieger

University of Nebraska-Lincoln, Lincoln, USA

A. Godshalk, C. Harrington, I. Iashvili, A. Kharchilava, C. Mclean, D. Nguyen, A. Parker, S. Rappoccio, B. Roozbahani

State University of New York at Buffalo, Buffalo, USA

G. Alverson, E. Barberis, C. Freer, Y. Haddad, A. Hortiangtham, G. Madigan, D.M. Morse, T. Orimoto, L. Skinnari, A. Tishelman-Charny, T. Wamorkar, B. Wang, A. Wisecarver, D. Wood

Northeastern University, Boston, USA

S. Bhattacharya, J. Bueghly, T. Gunter, K.A. Hahn, N. Odell, M.H. Schmitt, K. Sung, M. Trovato, M. Velasco

Northwestern University, Evanston, USA

R. Bucci, N. Dev, R. Goldouzian, M. Hildreth, K. Hurtado Anampa, C. Jessop, D.J. Karmgard, K. Lannon, W. Li, N. Loukas, N. Marinelli, I. Mcalister, F. Meng, C. Mueller, Y. Musienko³⁶, M. Planer, R. Ruchti, P. Siddireddy, G. Smith, S. Taroni, M. Wayne, A. Wightman, M. Wolf, A. Woodard

University of Notre Dame, Notre Dame, USA

J. Alimena, B. Bylsma, L.S. Durkin, S. Flowers, B. Francis, C. Hill, W. Ji, A. Lefeld, T.Y. Ling, B.L. Winer

The Ohio State University, Columbus, USA

S. Cooperstein, G. Dezoort, P. Elmer, J. Hardenbrook, N. Haubrich, S. Higginbotham, A. Kalogeropoulos, S. Kwan, D. Lange, M.T. Lucchini, J. Luo, D. Marlow, K. Mei, I. Ojalvo, J. Olsen, C. Palmer, P. Piroué, J. Salfeld-Nebgen, D. Stickland, C. Tully, Z. Wang

Princeton University, Princeton, USA

S. Malik, S. Norberg

University of Puerto Rico, Mayaguez, USA

A. Barker, V.E. Barnes, S. Das, L. Gutay, M. Jones, A.W. Jung, A. Khatiwada, B. Mahakud, D.H. Miller, G. Negro, N. Neumeister, C.C. Peng, S. Piperov, H. Qiu, J.F. Schulte, J. Sun, F. Wang, R. Xiao, W. Xie

Purdue University, West Lafayette, USA

T. Cheng, J. Dolen, N. Parashar

Purdue University Northwest, Hammond, USA

K.M. Ecklund, S. Freed, F.J.M. Geurts, M. Kilpatrick, Arun Kumar, W. Li, B.P. Padley, R. Redjimi, J. Roberts, J. Rorie, W. Shi, A.G. Stahl Leiton, Z. Tu, A. Zhang

Rice University, Houston, USA

A. Bodek, P. de Barbaro, R. Demina, Y.t. Duh, J.L. Dulemba, C. Fallon, T. Ferbel, M. Galanti, A. Garcia-Bellido, J. Han, O. Hindrichs, A. Khukhunaishvili, E. Ranken, P. Tan, R. Taus

University of Rochester, Rochester, USA

B. Chiarito, J.P. Chou, Y. Gershtein, E. Halkiadakis, A. Hart, M. Heindl, E. Hughes, S. Kaplan, S. Kyriacou, I. Laflotte, A. Lath, R. Montalvo, K. Nash, M. Osherson, H. Saka, S. Salur, S. Schnetzer, D. Sheffield, S. Somalwar, R. Stone, S. Thomas, P. Thomassen

Rutgers, The State University of New Jersey, Piscataway, USA

H. Acharya, A.G. Delannoy, J. Heideman, G. Riley, S. Spanier

University of Tennessee, Knoxville, USA

O. Bouhali⁷², A. Celik, M. Dalchenko, M. De Mattia, A. Delgado, S. Dildick, R. Eusebi, J. Gilmore, T. Huang, T. Kamon⁷³, S. Luo, D. Marley, R. Mueller, D. Overton, L. Perniè, D. Rathjens, A. Safonov

Texas A&M University, College Station, USA

N. Akchurin, J. Damgov, F. De Guio, S. Kunori, K. Lamichhane, S.W. Lee, T. Mengke, S. Muthumuni, T. Peltola, S. Undleeb, I. Volobouev, Z. Wang, A. Whitbeck

Texas Tech University, Lubbock, USA

S. Greene, A. Gurrola, R. Janjam, W. Johns, C. Maguire, A. Melo, H. Ni, K. Padeken, F. Romeo, P. Sheldon, S. Tuo, J. Velkovska, M. Verweij

Vanderbilt University, Nashville, USA

M.W. Arenton, P. Barria, B. Cox, G. Cummings, R. Hirosky, M. Joyce, A. Ledovskoy, C. Neu, B. Tannenwald, Y. Wang, E. Wolfe, F. Xia

University of Virginia, Charlottesville, USA

R. Harr, P.E. Karchin, N. Poudyal, J. Sturdy, P. Thapa, S. Zaleski

Wayne State University, Detroit, USA

J. Buchanan, C. Caillol, D. Carlsmith, S. Dasu, I. De Bruyn, L. Dodd, B. Gomber⁷⁴, M. Grothe, M. Herndon, A. Hervé, U. Hussain, P. Klabbers, A. Lanaro, K. Long, R. Loveless, T. Ruggles, A. Savin, V. Sharma, W.H. Smith, N. Woods

University of Wisconsin–Madison, Madison, WI, USA

[†] Deceased.

¹ Also at Vienna University of Technology, Vienna, Austria.

² Also at IRFU, CEA, Université Paris-Saclay, Gif-sur-Yvette, France.

³ Also at Universidade Estadual de Campinas, Campinas, Brazil.

⁴ Also at Federal University of Rio Grande do Sul, Porto Alegre, Brazil.

⁵ Also at Universidade Federal de Pelotas, Pelotas, Brazil.

- ⁶ Also at Université Libre de Bruxelles, Bruxelles, Belgium.
- ⁷ Also at University of Chinese Academy of Sciences, Beijing, China.
- ⁸ Also at Institute for Theoretical and Experimental Physics named by A.I. Alikhanov of NRC 'Kurchatov Institute', Moscow, Russia.
- ⁹ Also at Joint Institute for Nuclear Research, Dubna, Russia.
- ¹⁰ Also at Cairo University, Cairo, Egypt.
- ¹¹ Also at Helwan University, Cairo, Egypt.
- ¹² Now at Zewail City of Science and Technology, Zewail, Egypt.
- ¹³ Also at Purdue University, West Lafayette, USA.
- ¹⁴ Also at Université de Haute Alsace, Mulhouse, France.
- ¹⁵ Also at CERN, European Organization for Nuclear Research, Geneva, Switzerland.
- ¹⁶ Also at RWTH Aachen University, III. Physikalisches Institut A, Aachen, Germany.
- ¹⁷ Also at University of Hamburg, Hamburg, Germany.
- ¹⁸ Also at Brandenburg University of Technology, Cottbus, Germany.
- ¹⁹ Also at Institute of Physics, University of Debrecen, Debrecen, Hungary.
- ²⁰ Also at Institute of Nuclear Research ATOMKI, Debrecen, Hungary.
- ²¹ Also at MTA-ELTE Lendület CMS Particle and Nuclear Physics Group, Eötvös Loránd University, Budapest, Hungary.
- ²² Also at Indian Institute of Technology Bhubaneswar, Bhubaneswar, India.
- ²³ Also at Institute of Physics, Bhubaneswar, India.
- ²⁴ Also at Shoolini University, Solan, India.
- ²⁵ Also at University of Visva-Bharati, Santiniketan, India.
- ²⁶ Also at Isfahan University of Technology, Isfahan, Iran.
- ²⁷ Also at Plasma Physics Research Center, Science and Research Branch, Islamic Azad University, Tehran, Iran.
- ²⁸ Also at Italian National Agency for New Technologies, Energy and Sustainable Economic Development, Bologna, Italy.
- ²⁹ Also at Centro Siciliano di Fisica Nucleare e di Struttura della Materia, Catania, Italy.
- ³⁰ Also at Università degli Studi di Siena, Siena, Italy.
- ³¹ Also at Scuola Normale e Sezione dell'INFN, Pisa, Italy.
- ³² Also at Riga Technical University, Riga, Latvia.
- ³³ Also at Malaysian Nuclear Agency, MOSTI, Kajang, Malaysia.
- ³⁴ Also at Consejo Nacional de Ciencia y Tecnología, Mexico City, Mexico.
- ³⁵ Also at Warsaw University of Technology, Institute of Electronic Systems, Warsaw, Poland.
- ³⁶ Also at Institute for Nuclear Research, Moscow, Russia.
- ³⁷ Now at National Research Nuclear University 'Moscow Engineering Physics Institute' (MEPhI), Moscow, Russia.
- ³⁸ Also at St. Petersburg State Polytechnical University, St. Petersburg, Russia.
- ³⁹ Also at University of Florida, Gainesville, USA.
- ⁴⁰ Also at P.N. Lebedev Physical Institute, Moscow, Russia.
- ⁴¹ Also at California Institute of Technology, Pasadena, USA.
- ⁴² Also at Budker Institute of Nuclear Physics, Novosibirsk, Russia.
- ⁴³ Also at Faculty of Physics, University of Belgrade, Belgrade, Serbia.
- ⁴⁴ Also at University of Belgrade, Belgrade, Serbia.
- ⁴⁵ Also at INFN Sezione di Pavia^a, Università di Pavia^b, Pavia, Italy.
- ⁴⁶ Also at National and Kapodistrian University of Athens, Athens, Greece.
- ⁴⁷ Also at Universität Zürich, Zurich, Switzerland.
- ⁴⁸ Also at Stefan Meyer Institute for Subatomic Physics (SMI), Vienna, Austria.
- ⁴⁹ Also at Adiyaman University, Adiyaman, Turkey.
- ⁵⁰ Also at Sirtak University, SIRTAK, Turkey.
- ⁵¹ Also at Beykent University, Istanbul, Turkey.
- ⁵² Also at Istanbul Aydin University, Istanbul, Turkey.
- ⁵³ Also at Mersin University, Mersin, Turkey.
- ⁵⁴ Also at Piri Reis University, Istanbul, Turkey.
- ⁵⁵ Also at Gaziosmanpasa University, Tokat, Turkey.
- ⁵⁶ Also at Ozyegin University, Istanbul, Turkey.
- ⁵⁷ Also at Izmir Institute of Technology, Izmir, Turkey.
- ⁵⁸ Also at Marmara University, Istanbul, Turkey.
- ⁵⁹ Also at Kafkas University, Kars, Turkey.
- ⁶⁰ Also at Istanbul University, Istanbul, Turkey.
- ⁶¹ Also at Istanbul Bilgi University, Istanbul, Turkey.
- ⁶² Also at Hacettepe University, Ankara, Turkey.
- ⁶³ Also at School of Physics and Astronomy, University of Southampton, Southampton, United Kingdom.
- ⁶⁴ Also at Rutherford Appleton Laboratory, Didcot, United Kingdom.
- ⁶⁵ Also at Institute for Particle Physics Phenomenology Durham University, Durham, United Kingdom.
- ⁶⁶ Also at Monash University, Faculty of Science, Clayton, Australia.
- ⁶⁷ Also at Bethel University, St. Paul, USA.
- ⁶⁸ Also at Karamanoğlu Mehmetbey University, Karaman, Turkey.
- ⁶⁹ Also at Bingol University, Bingol, Turkey.
- ⁷⁰ Also at Sinop University, Sinop, Turkey.
- ⁷¹ Also at Mimar Sinan University, Istanbul, Istanbul, Turkey.
- ⁷² Also at Texas A&M University at Qatar, Doha, Qatar.
- ⁷³ Also at Kyungpook National University, Daegu, Republic of Korea.
- ⁷⁴ Also at University of Hyderabad, Hyderabad, India.